

Organic & Biomolecular Chemistry

www.rsc.org/obc

Volume 11 | Number 11 | 21 March 2013 | Pages 1745–1908



ISSN 1477-0520

RSC Publishing

PAPER

Steven V. Ley *et al.*

An expeditious synthesis of imatinib and analogues utilising flow chemistry methods



1477-0520 (2013) 11:11;1-F

PAPER

An expeditious synthesis of imatinib and analogues
utilising flow chemistry methods†

Cite this: *Org. Biomol. Chem.*, 2013, **11**,
1822

Mark D. Hopkin,^a Ian R. Baxendale^b and Steven V. Ley^{*a}

Received 15th October 2012,
Accepted 4th December 2012

DOI: 10.1039/c2ob27002a

www.rsc.org/obc

A flow-based route to imatinib, the API of Gleevec, was developed and the general procedure then used to generate a number of analogues which were screened for biological activity against Abl1. The flow synthesis required minimal manual intervention and was achieved despite the poor solubility of many of the reaction components.

Introduction

Currently the hit to lead and lead optimisation procedures in the development of active pharmaceutical ingredients (APIs) involve many labour intensive and time consuming processes. Often a large number of analogues of the initial hit compound will be synthesised in batch-mode, purified and then sent for screening. Multi-step operations such as these require individual reaction control, optimisation, work-up and purification techniques which are only achievable in dedicated and expensive facilities. When the compounds have been isolated, they are usually transferred to an alternative workforce for screening. After analysis of these data and a refinement of the models used, a decision can be made as to which compounds, if any, can be taken forward for a further round of synthesis and screening. Overall in this process a large amount of time, materials and money can be wasted in producing redundant compounds.

Given the similarities in the structures of many of these analogues, a system capable of synthesising and screening compounds in one smooth operation would be of value if the biological data could be more rapidly used to iterate the next synthesis cycle.

Whilst flow chemistry can offer many benefits in the preparation of functional molecules,¹ only a few examples of sequential multi-step flow synthesis have been described.² This is inevitably due to the complexity of the experimental set-up and the systems involved. Our group has been

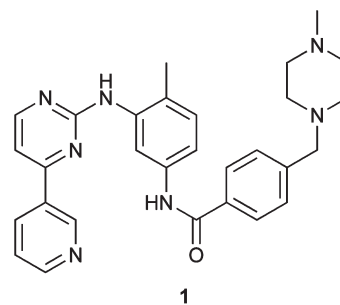


Fig. 1 Structure of imatinib (1).

interested in developing technology^{3,4} to overcome the problems encountered in multi-step flow synthesis. Consequently we sought to develop a flow-based route to a known pharmaceutical agent that avoided the typical manual handling of intermediates and could potentially be coupled to a future screening platform.

Imatinib (1) (Fig. 1) is a tyrosine kinase inhibitor developed by Novartis AG and is used for the treatment of chronic myeloid leukaemia (CML) and gastrointestinal stromal tumours.^{5,6} It is currently produced by Novartis under the brand name Gleevec as the mesylate salt. Both small- and large-scale routes to imatinib involve many insoluble intermediates.⁷ Therefore we saw the preparation of 1 as a particularly challenging test for flow chemistry technologies, but one which was ultimately successful and also led to a small collection of useful analogues.

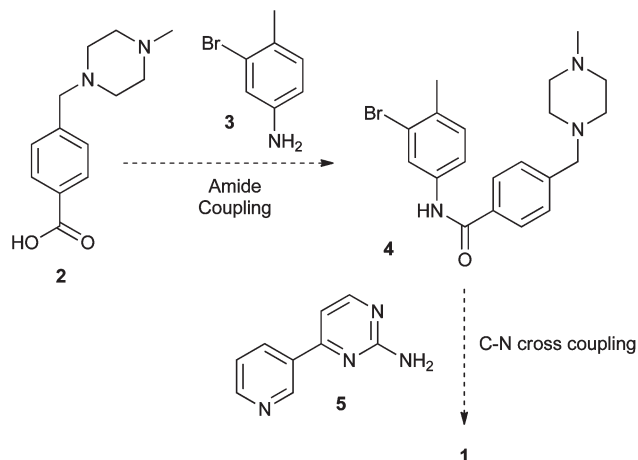
Results and discussion

The nitro- and guanidine-substituted materials used in many batch syntheses of imatinib were deemed unsuitable for a flow synthesis owing to known solubility issues. We therefore devised a strategy for the synthesis of 1 which avoided these

^aDepartment of Chemistry, University of Cambridge, Lensfield Road, Cambridge, CB2 1EW, UK. E-mail: svl1000@cam.ac.uk

^bDepartment of Chemistry, Durham University, South Road, Durham, DH1 3LE, UK. E-mail: i.r.baxendale@durham.ac.uk

†Electronic supplementary information (ESI) available: Full experimental details for the synthesis of all intermediates and final compounds, NMR assignments for all compounds and NMR spectra of final compounds. See DOI: 10.1039/c2ob27002a

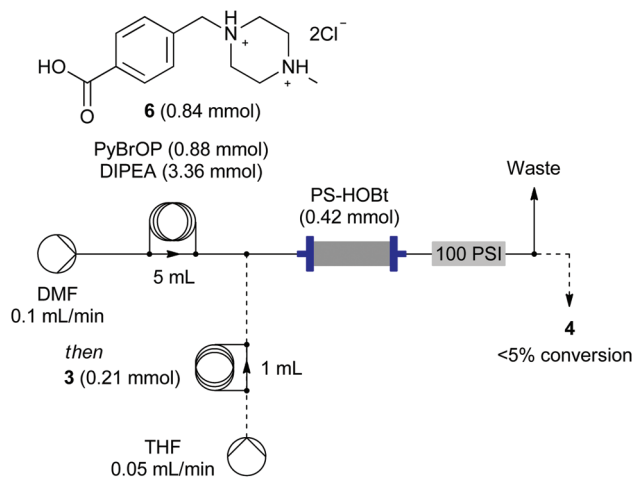


Scheme 1 Planned route to 1.

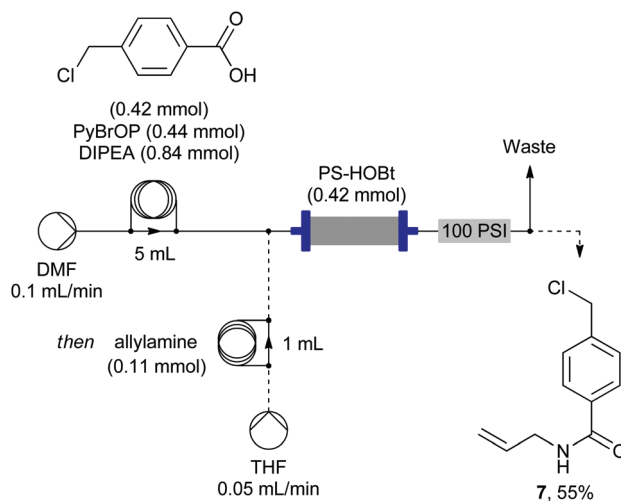
intermediates (Scheme 1). Amide 4 was selected as an initial synthesis target as this was likely to be more soluble due to the piperazine moiety and could be formed by a coupling between 3-bromo-4-methylaniline and amino acid 2 in a similar fashion to known procedures.⁸ The final step of the synthesis would then comprise of a cross-coupling between amide 4 and 5 to yield imatinib (1).

During our flow synthesis of the neolignan natural product grossamide⁸ we demonstrated that flowing a solution of carboxylic acid, PyBrOP and DIPEA in DMF through a cartridge packed with a polymer-supported HOBt resin led to the formation of a supported active ester. The supported active ester could then be reacted with an amine by passage through the column to afford the required amide. The exiting stream was subsequently eluted through an additional column containing polymer-supported sulfonic acid to remove any excess amine therefore leading to a purified amide product flow stream.

The salt 6 was available by chloride displacement of 4-(chloromethyl)benzoic acid with *N*-methylpiperazine.⁹ The flow reactor configuration initially devised (Scheme 2) called for the introduction of the salt 6 together with PyBrOP and DIPEA *via* an injection loop into a DMF solvent flow line. It was determined that a large excess of base was needed to effect full deprotonation. This was further complicated by the necessity to employ several equivalents of 6 to completely saturate the PS-HOBt column. After flushing with additional anhydrous DMF to remove impurities and a final elution with dry THF, we assumed the column now contained the supported HOBt active ester. However after injection of the 3-bromo-4-methylaniline coupling partner, LC-MS indicated that only a ~5% conversion to the desired product 4 had occurred. Suspecting the relatively poor nucleophilicity of the aniline to be the cause, we repeated the experiment replacing this with allylamine as a more nucleophilic primary amine. Once again, analysis of the reactor output showed poor conversion from the starting material to the amide (<15% by LC-MS) and the presence of other impurities.



Scheme 2 Attempted formation of 4 using PS-HOBt methodology.

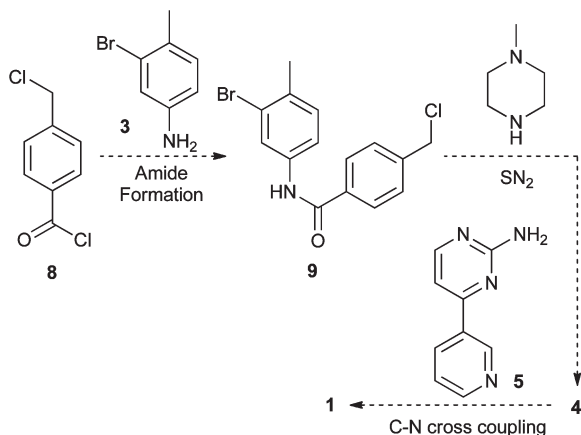


Scheme 3 Formation of test amide 7.

We reasoned that the basicity of the *N*-methylpiperazine ring in 6 may be responsible for the lower than expected conversions. Accordingly we decided to modify the strategy and initially investigated the model system of coupling 4-(chloromethyl)benzoic acid with allylamine as depicted in Scheme 3. Although pleasingly we obtained a 55% yield of the amide 7, when we used the real 3-bromo-4-methylaniline as a substrate, only a poor 20% conversion to the amide 9 was realised. This indicated that our main issue was actually one of inherent reactivity. The low nucleophilicity of the aniline combined with the commonly-encountered problem of reduced reactivity of immobilised reagents made this reaction problematic.

Solution-based synthesis of 9

The failure of the above polymer-supported strategy in flow led us to explore a solution phase method. Given the insolubility of compound 6 in most organic solvents we decided to reverse the sequence and begin with the commercially available



Scheme 4 Revised strategy for the formation of **1**.

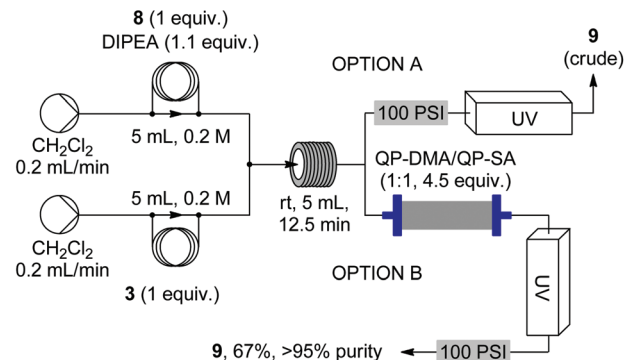
4-(chloromethyl)benzoyl chloride (**8**) as an alternative coupling partner to form **9**. Upon chloride displacement with *N*-methylpiperazine, this would result in amide **4** and a final bromide displacement would lead to **1** (Scheme 4).

In practice, this was not as straightforward as it may seem. While in batch mode the formation of an amide from an acid chloride and aniline is straightforward since insolubility is not a concern, in flow the generation of hydrochloric acid, and hence insoluble salts that potentially could block the reactor, is a significant concern – therefore the selection of base and solvent is critical. A rapid batch screen of solvents and bases (Table 1) used for the amide formation of **9** was therefore carried out. It was initially hoped that the reaction could be performed without addition of a solution phase base such that post reaction scavenging of the generated HCl could be performed. Unfortunately, in both MeCN and CH₂Cl₂ a precipitate corresponding to the aniline hydrochloride salt was immediately generated when the acid chloride was added to the solution. The amide formation was also conducted in DMF as the solvent to increase the solubility of the aniline hydrochloride salt and thus allow the reaction to be performed using polystyrene-supported dimethylamine (QP-DMA). However, the

Table 1 Screening of solvents and bases for the formation of **9**

$\text{8 (1 equiv.)} + \text{3 (1 equiv.)} \xrightarrow[\text{Solvent, rt, 1 h}]{\text{Base (1.1 equiv.)}} \text{9}$			
Entry	Solvent	Base	Notes ^a
1	MeCN	—	Precipitate on addition of 8
2	MeCN	NEt ₃	Precipitate formed after 30 min
3	MeCN	QP-DMA	Precipitate on addition of 8
4	CH ₂ Cl ₂	—	Precipitate on addition of 8
5	CH ₂ Cl ₂	NEt ₃	100% conversion, cloudy reaction mixture
6	CH ₂ Cl ₂	QP-DMA	Precipitate on addition of 8
7	CH ₂ Cl ₂	(<i>i</i> -Pr) ₂ NEt	100% conversion
8	DMF	—	Formamidine generated
9	DMF	NEt ₃	Formamidine generated
10	DMF	QP-DMA	Formamidine generated

^a Conversion measured by LC-MS.



Scheme 5 Formation of **9**. (A) As crude with UV detector after BPR. (B) In high purity by using PS scavengers.

corresponding dimethyl formamidine was also formed in 50% yield as a major by-product.

This preliminary screen implied that a solution phase base would indeed be necessary in order to conduct the sequence in flow. The amide formation in the presence of triethylamine proceeded well in both CH₂Cl₂ and MeCN, but once again **9** precipitated from the MeCN solution. The use of triethylamine in CH₂Cl₂ led to 100% conversion to the product as a cloudy solution. This cloudiness could be eliminated by the replacement of triethylamine with DIPEA resulting in a more soluble hydrochloride salt.

We therefore chose DIPEA as the base in CH₂Cl₂ as the most suitable conditions for the flow experiments (Scheme 5A). In this reactor setup, a UV detector was used to determine when the reaction mixture was exiting the system and thus provide a first level of analysis. The output stream was directed into flasks containing MeOH to quench any unreacted acid chloride ensuring that the reaction occurred exclusively in the flow system.

The UV readout of the reactor output is shown in Fig. 2 (top). The spiking in this figure is likely due to air bubbles in the reaction stream formed as a result of the depressurisation of the solution as it passes through the back-pressure regulator (BPR). LC-MS analysis of the fractionated reactor output indicated that complete conversion to **9** had occurred during the steady-state period. The output of the flow-stream at this point also contained excess DIPEA and the corresponding hydrochloride salt hence an in-line work-up procedure was required (Scheme 5B). The removal of these components was achieved by passing the output stream through a column packed with a mixture of polystyrene-supported dimethylamine (4.5 equivalents) and polystyrene-supported sulfonic acid (4.5 equivalents). The supported base deprotonates the DIPEA hydrochloride salt liberating DIPEA which was then captured by the sulfonic acid resin. The use of lower stoichiometries of the supported scavengers resulted in small quantities of the DIPEA hydrochloride salt passing through without capture. The ability to combine two functionalities that would interact in solution in the same scavenging column is a useful feature of these polymer-supported reagents.

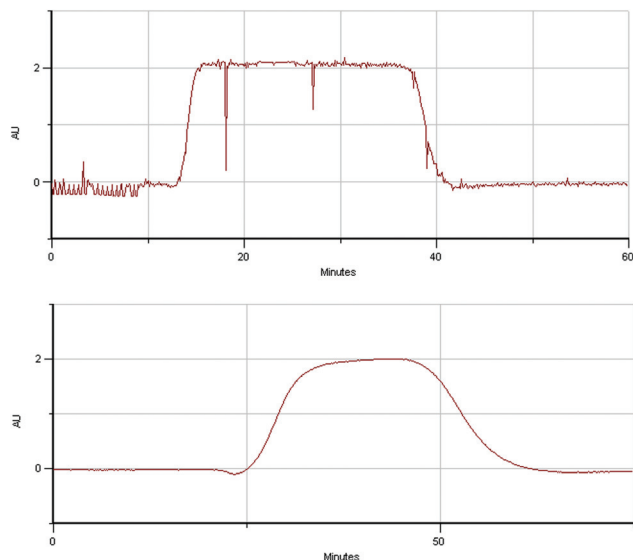


Fig. 2 UV (340 nm) trace of reactor output. Top: set-up as shown in Scheme 5A. Bottom: set-up as shown in Scheme 5B.

In order to observe the effect of the scavenging column, the UV detector was then placed in-line to monitor the process. In this setup, the BPR was placed after the UV detector to minimise the spiking problems. The reagents were injected in an identical manner to the previous experiment to give the product **9** in 67% yield and excellent (>95%) purity. The non-quantitative yield can be attributed to loss of material through injection using a sample loop and chromatographic effects of the immobilised reagents. The output profile from the reactor is shown at the bottom of Fig. 2. This indicates that the product elutes over 35 min compared to the 25 min theoretical length of the injection slug. This increased dispersion is caused by diffusion and mixing as the product passes through the reactor and occurs to a much larger extent when the stream passes through a column of polymer-supported reagent.⁴

Synthesis of amide **4**

The planned flow synthesis of **4** from **9** involves a nucleophilic displacement of the benzylic chloride of **9** with *N*-methylpiperazine assisted by passing the reagents through a polymer-supported base. Next, the flow stream would be directed through a cartridge containing a polymer-supported electrophilic reagent to selectively remove any unreacted secondary amine. This would be followed by a supported acid to catch the basic product as its conjugate acid, permitting any unreacted **9** to continue to waste. The release of compound **4** would be achieved by passing a solution phase base through the column which following solvent removal would yield the purified product.

Since the previous flow step for the generation of amide **9** had been performed in CH_2Cl_2 , it was hoped that this next stage could also be conducted in the same solvent allowing for a continuous integrated process. To investigate the potential of

Table 2 Screening of stoichiometry of *N*-methylpiperazine in the formation of **4**

Entry	Equiv. of <i>N</i> -methylpiperazine	Temperature ^a (°C)	Time (h)	Notes ^b	Conditions	
					9 (1 equiv.) + <i>N</i> -methylpiperazine	0.05 M, 1:1 $\text{CH}_2\text{Cl}_2/\text{DMF}$ → 4
1	1.5	100	1.5	70% conversion (50% after 0.5 h)		
2	2	120	0.5	80% conversion		
3	3	120	0.5	95% conversion		

^a Heating performed by MW irradiation. ^b Conversion measured by LC-MS.

this unification, a 0.05 M (a similar concentration to that achieved in the output solution of the first step) solution of **9** and *N*-methylpiperazine (1.5 equivalents) in CH_2Cl_2 was heated at 100 °C for 1 h. A residue was formed on the side of the reaction flask that was shown by LC-MS analysis to correspond to the product. The insolubility of **4** therefore suggested that the use of CH_2Cl_2 as the solvent in flow would not be appropriate.

Since a further flow stream containing the *N*-methylpiperazine was being introduced, a second solvent more able to solubilise the product (**4**) could be added. As an alcohol would not be suitable because of subsequent incompatibility with the electrophilic scavenger planned for sequestering the excess *N*-methylpiperazine, DMF was instead chosen. The reaction was first attempted in batch (Table 2) at elevated temperature to drive the reaction to completion. A fast reaction would enable the step to be performed readily in flow.

The results show that increasing the number of equivalents of *N*-methylpiperazine increases the rate of reaction and improves the overall conversion. However, any excess *N*-methylpiperazine would need to be scavenged from solution after the reaction. A two equivalent excess was selected as the best compromise since a small increase in yield would be counteracted with a large increase in the amount of scavenging resin required. With this in mind, the reaction was translated to flow using a 1 : 1 mixture of CH_2Cl_2 -DMF at 0.03 M, a slightly reduced concentration since the addition of DMF would reduce the concentration of the output stream from the previous step. The results (Table 3) indicated that doubling the reaction time led to an increase in conversion of only 10% suggesting that much longer reaction times would be required to obtain complete conversion to **4**. Interestingly, using a higher temperature of 130 °C had little effect on the reaction. The addition of a catalytic quantity of iodide in the form of TBAI also had no impact on overall conversion.

As no base had been added to the reaction mixture, both the product and remaining *N*-methylpiperazine will be protonated to some extent by the HCl generated in the reaction thus reducing the concentration of free amine and thereby inhibiting the reaction. In addition, deprotonation of the *N*-methylpiperazine would be required in order for it to be effectively

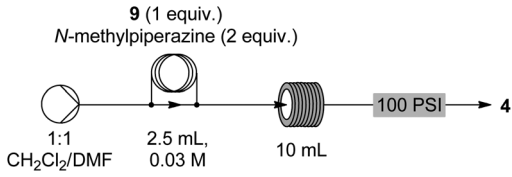
scavenged. To address this issue and in an attempt to drive the reaction to completion the reaction was repeated in the presence of a number of solid-supported bases (Table 4).¹⁰

When the reactions were conducted in the presence of PS-carbonate as a solid base, the corresponding benzyl alcohol was formed as a major byproduct. This side reaction did not occur when PS-BEMP or PS-TBD were employed. Using elevated temperatures (100 °C) caused discolouration of the reaction mixture hence an optimum temperature of 80 °C was used in subsequent reactions. Ultimately, the conditions in entry 8, Table 4 were found to give the highest conversion to **4** and so were transcribed to flow (Scheme 6). A total of 6 equivalents of PS-TBD were used to provide a suitable residence time in the column. Purification was achieved by directing the output of the PS-TBD cartridge through a column of polymer-supported isocyanate (3 equivalents) to scavenge the excess *N*-methylpiperazine. This resin was chosen since it is a good electrophile and is available as a macroporous resin that is easy to pack into a column and does not swell upon solvation. The output from this column was then directed into a column filled with QP-SA (6 equivalents) to catch the product from unreacted **9** which passed to waste. Analysis of the output

stream showed there to be no product **4** present. Following a wash of the resin with MeOH to elute the DMF, a solution of NH₃ in MeOH was passed through the column to release product **4** in 56% yield and >95% purity following solvent removal. The yield here was slightly lower than expected and can partly be attributed to incomplete elution of the product from the resins in the procedure, for example Fig. 3, bottom trace shows that the UV absorption of the flow stream takes a relatively long period to reach the baseline. Crucially no *N*-methylpiperazine was observed in the output before or after solvent removal.

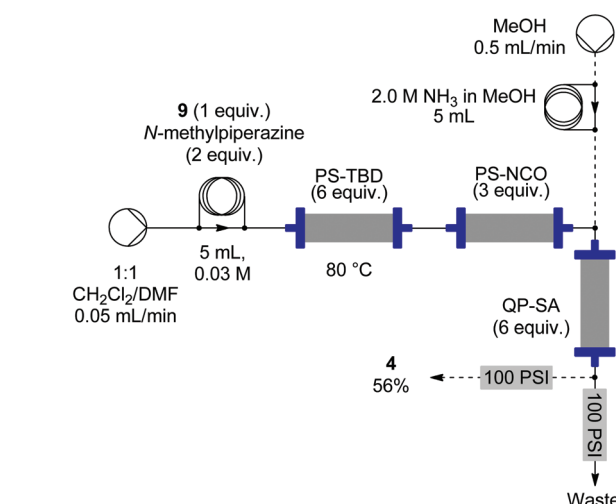
To improve the diagnostic visualisation of the process the UV trace of the output from the PS-TBD column was measured by placing a UV detector in-line and is shown in Fig. 3, top trace. This indicates a column residence time of only 12 min. Interestingly, the plot shows an increase in the output concentration during the “steady-state” period. HPLC analysis of the reaction mixture at 20 and 125 min after injection indicated conversions of 89% and 83% respectively suggesting that the UV profile may be due to the column of PS-TBD becoming

Table 3 Effect of temperature and time on the flow synthesis of **4**



Entry	Flow rate (mL min ⁻¹)	Coil temperature (°C)	Residence time (min)	Conversion ^a (%)
1	0.3	120	33	62
2 ^b	0.3	120	33	61
3	0.3	130	33	61
4	0.15	120	67	68
5	0.15	130	67	71

^a Conversion measured by HPLC. ^b 5 mol% TBAI added to solution.



Scheme 6 Flow synthesis and purification of **4** with PS-TBD.

Table 4 Screening of polymer-supported bases in the formation of **4**

Entry	Base	Equiv. of base	Conditions		Conversion ^b (%)
			Temperature ^a (°C)	Time (h)	
$\begin{array}{c} \mathbf{9} \text{ (1 equiv.)} \\ + \\ \text{N-methylpiperazine (2 equiv.)} \end{array} \xrightarrow{\text{0.03 M, 1:1 CH}_2\text{Cl}_2/\text{DMF}} \mathbf{4}$					
1	PS-BEMP	2	100	0.5	Sequestered SM and product
2	PS-CO ₃	2	60	0.5	67 (13 to benzyl alcohol)
3	PS-CO ₃	2	60	1	76 (14 to benzyl alcohol)
4	PS-TBD	1	60	0.5	68
5	PS-TBD	1	100	0.5	79
6	PS-TBD	2	60	0.5	88
7	PS-TBD	2	80	0.5	94
8	PS-TBD	2	80	1	97

^a Heating performed by MW irradiation. ^b Conversion measured by HPLC.

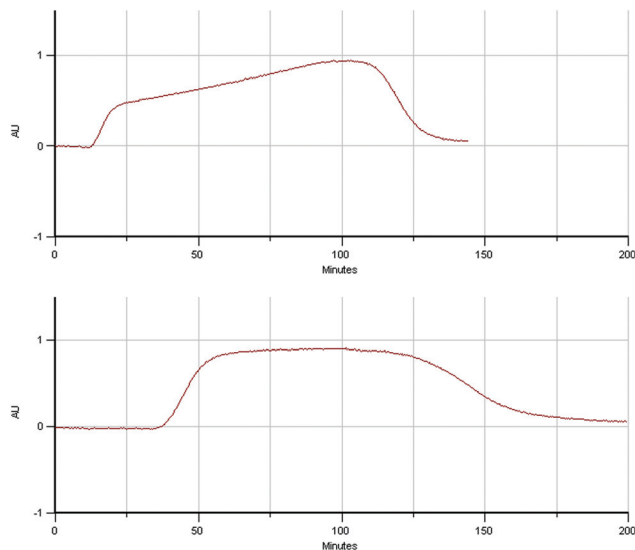


Fig. 3 UV (340 nm) traces before (top) and after (bottom) PS-NCO.

more protonated over time, resulting in a lower availability of free-base. Positioning the UV detector after the PS-NCO column showed that further dispersion occurs as the material passes through this additional column (Fig. 3, bottom trace).

Given the relatively high commercial expense of PS-TBD used in the formation of **4**, only small quantities could be realistically used resulting in a short retention time inside the heated reactor (Scheme 6). Alternatively solid, powdered K_2CO_3 could be packed into a column and used in flow since it is only sparingly soluble in the solvents used. As it is inexpensive, a large excess and hence longer retention time could be achieved without the need for very low flow rates. It was hoped the longer retention time would allow the reaction to proceed closer to completion. This indeed proved to be the case resulting in a conversion of 80% when the reaction shown in Scheme 6 was repeated with a column of K_2CO_3 (5.2 g) in place of the PS-TBD at a flow rate of 0.1 mL min^{-1} . A retention time of 30 min in the basic column was obtained which is a significant improvement on the original 12 min achieved using PS-TBD.

Combining the steps

Our next task was to combine the amide formation and benzyl chloride displacement into a single integrated process avoiding the manual transfer and handling of intermediate **9**. Ideally, this would be achieved by the direct introduction of a third stream containing *N*-methylpiperazine to the output of the first step. The third pump could in principle have been triggered by the UV detection of the output solution from the first step. However, a drawback of using a scavenging cartridge for purification is that the reactor does not reach steady-state conditions very quickly and the output concentration varies considerably with time (Fig. 3). Since the flow rate and concentration of the third stream remains constant, the *N*-methylpiperazine would be in significant excess during the rising and falling periods of the output of the first step; an undesirable

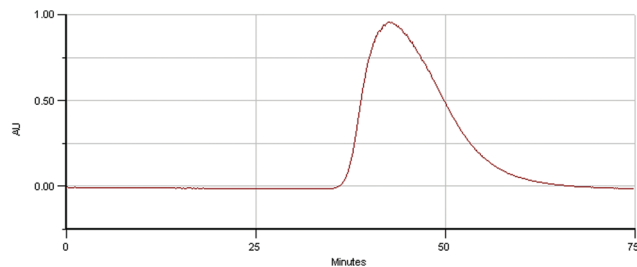
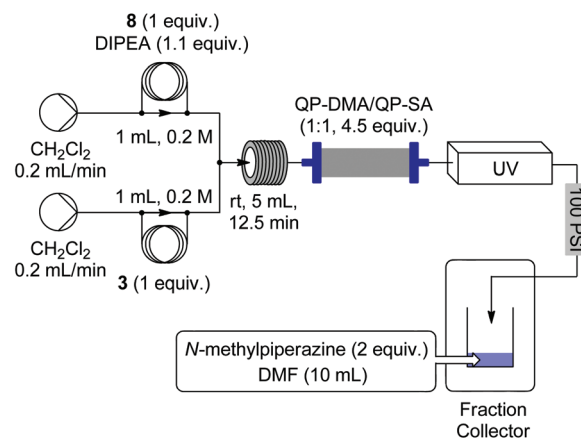


Fig. 4 UV (340 nm) trace of scaled down formation of **9**.

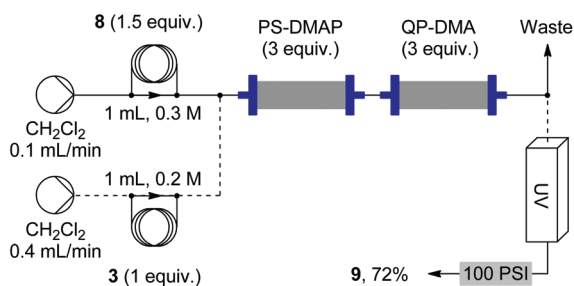
situation since this excess must be scavenged from solution by the relatively expensive isocyanate resin. To overcome this issue, an alternative strategy was envisaged in which the entire peak would be temporarily collected into a vessel already containing the *N*-methylpiperazine in a DMF solution thus forming a homogeneous solution of known concentration ready for injection into the next step. It was anticipated that this could be easily achieved using a UV controlled fraction collector followed by automatic aspiration and injection into the subsequent step.

The previous procedure described in Scheme 5B was scaled down by a factor of five to enable the output to be conveniently collected in a 20 mL fraction collector vial (although in principle multiple vials could be used with further re-injections). This reaction set-up resulted in the formation of **9** in improved yield (78%) and excellent purity (>95%). The UV trace of the output from the first step of the sequence (Fig. 4) showed that the system did not reach a steady-state condition as before (Fig. 2) and that the majority of the product was distributed over a 25 min period (equating to a 10 mL internal volume). Collection of this peak into a vial already containing 10 mL of *N*-methylpiperazine (2 equivalents) in DMF generated a combined 20 mL 1 : 1 CH_2Cl_2 -DMF solution of **9** and *N*-methylpiperazine (Scheme 7).

When this solution was injected into the reactor (Scheme 6) the conversion to **4** was only 20% highlighting the high concentration dependence of the reaction. In an attempt to



Scheme 7 UV triggered collection of **9** into a receptacle containing *N*-methylpiperazine in DMF.



Scheme 8 Flow formation of **9** using PS-DMAP.

increase the output concentration of **9**, the concentration of starting materials in the amide formation was increased by a factor of 5 (0.2 mL/1.0 M *cf.* 1 mL/0.2 M). Interestingly, the product output profile did not change substantially, only reducing the output volume to 8 mL (previously 10 mL) suggesting that the dispersion in the scavenging column was the limiting factor. Given the limited concentration of **9** that could be produced using this sequence, an alternative strategy was required in order to achieve acceptable yields of **4**.

PS-DMAP approach to the formation of **9**

An alternative approach was investigated in which **8** was pre-loaded onto PS-DMAP and then released by reaction with 3-bromo-4-methylaniline (Scheme 8). This general approach has previously been successfully used to prepare amides and sulfonamides¹¹ albeit not as a flow process. First a CH₂Cl₂ solution of acid chloride **8** (0.3 M) was loaded onto the PS-DMAP column. Subsequently the injection of the aniline was attempted at a concentration of 0.5 M, however the resultant product crystallised from solution at the outlet of the reactor and resulted in blocking of the system. The concentration was therefore reduced to 0.2 M. It was hoped that the use of excess PS-DMAP would capture any acid formed due to residual water. However in practice the output of the reactor gave a 3 : 1 mixture of **9** and hydrolysed **8**. Given that dry CH₂Cl₂ was used for the experiment, this residual water was attributed to the resin which is reported to be difficult to dry completely. To overcome this problem, a cartridge filled with QP-DMA was introduced to scavenge any carboxylic acid generated in the reaction. The product was then isolated in 72% yield and excellent purity (>95%) after solvent evaporation.

The trace in Fig. 5 shows the UV profile of the product stream monitored at the outlet of the reactor. The slight initial shoulder is due to low-level highly coloured aniline impurities which rapidly elute through the system. The resulting product distribution gave a significant improvement on the previous solution phase formation of compound **9**.

From the profile it is evident that the majority of the product is eluted in the first 10 min after it began to emerge from the reactor. Therefore a fraction collector was set to collect the product output at a defined absorption threshold in 10 min (4 mL) fractions. The first fraction corresponded to 75% of the total collected mass and hence this was used for the subsequent steps.

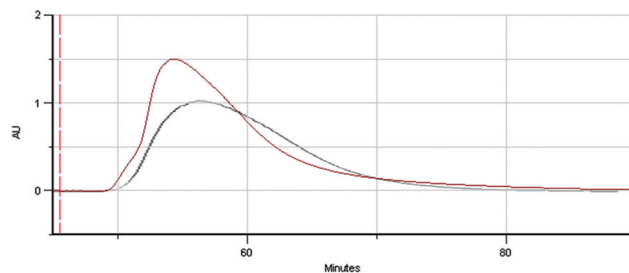


Fig. 5 UV (340 nm) trace of amide **9** formation using PS-DMAP (0.2 M solution phase formation of **9** overlaid in black).

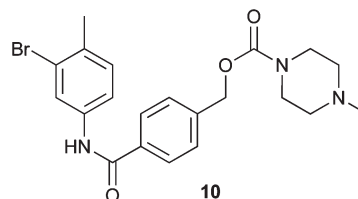


Fig. 6 Structure of **10**.

In a further effort to increase the concentration of **9** injected into the second step and thus the conversion to **4**, the amount of DMF in the collection flask was reduced to 2 mL, thus resulting in a 20 mM, 2 : 1 CH₂Cl₂-DMF solution which was injected at 0.1 mL min⁻¹ through a column of K₂CO₃ held at 80 °C resulting in 62% conversion as determined by ¹H NMR. This was interesting since the conversion obtained from a 1 : 1 CH₂Cl₂-DMF solution of similar concentration was greater (80%) suggesting the solvent has a pronounced effect on the reaction. The reaction was repeated with a 30 mM solution of **9** in neat DMF which gave a 95% conversion indicating that the presence of CH₂Cl₂ was actually inhibiting the reaction.

Greater investigation of the reactor output indicated an additional signal in the LC-MS spectrum of the reactor output that was initially missed as it coeluted with **4**. It was noted on reinspection that it was present in all reactions performed using K₂CO₃ but absent from the PS-TBD promoted reactions. We were able to isolate this substance in 9% yield from the flow reaction performed with neat DMF and showed it to be the carbamate **10** (Fig. 6).

A literature search revealed that similar carbamate formation is preceded when a carbon dioxide source is present.¹² CaCO₃ has a much lower solubility in water and so is less likely to liberate CO₂ under these conditions hence the reaction was repeated with a column packed with CaCO₃. This resulted in 95% conversion to the product without any formation of **10**. From these results indicating the detrimental effect of CH₂Cl₂, an in-line method of solvent removal was investigated.

Multiple methods currently exist for the in-line removal of solvents, for example the Biotage AB V10 solvent evaporator¹³ allows a flow stream to be directed into a heated, rotating vial

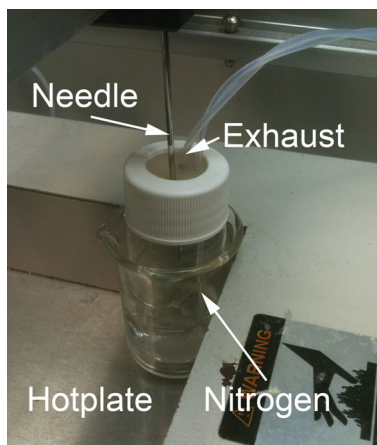


Fig. 7 In-line solvent evaporation.

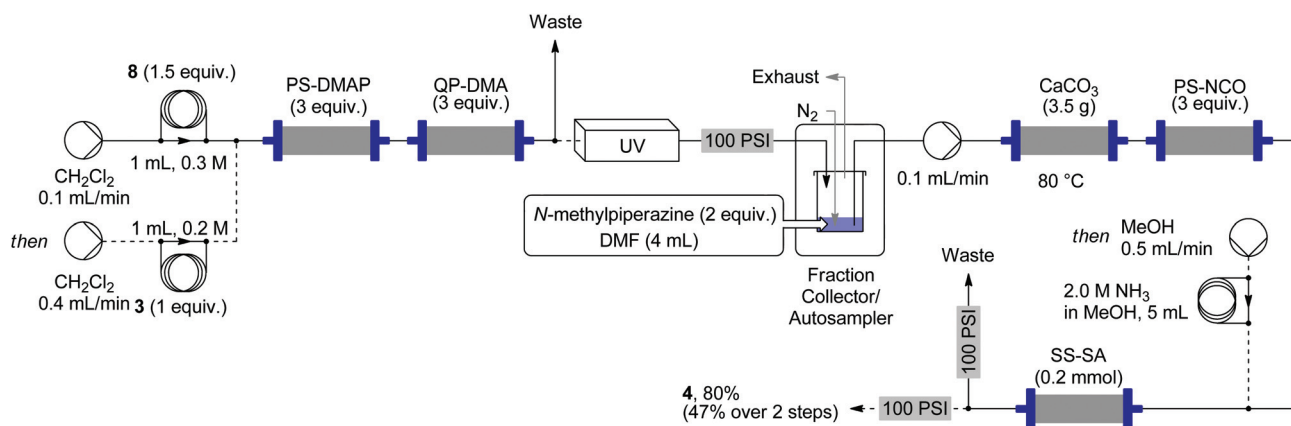
under reduced pressure to continuously evaporate the solvent. Dissolution of the residue is also possible, however further injection of the resultant solution into a second step without manual handling is only possible with complex, expensive robotic equipment.¹⁴ A simple in-line solution was therefore developed by positioning a vial capped with a rubber septum and venting tube on a hotplate to evaporate the volatile CH_2Cl_2 solvent as the output was collected (Fig. 7). The rate of evaporation was enhanced by directing an additional stream of nitrogen gas into the vial to displace the solvent vapours through an exhaust pipe. In this case, the DMF solvent and *N*-methylpiperazine are significantly less volatile than the CH_2Cl_2 hence they can be added to the vial prior to collection and removal of the CH_2Cl_2 without their loss. If transfer to a more volatile solvent was required, the second reagent and solvent could be automatically transferred to the vial by the fraction collector for dissolution after evaporation and prior to injection into the next step. As a simple approach this method avoids the need for manual solvent removal and handling of intermediate compounds.

Using the protocol described previously (Scheme 9), the first 4 mL fraction from the amide formation was

automatically collected into a vial containing *N*-methylpiperazine (2 equivalents based on the expected output) in DMF (4 mL) and the CH_2Cl_2 removed. This resulted in a 30 mM solution of **9** in DMF and 2 equivalents of *N*-methylpiperazine. Next the efficiency of the catch and release purification in the second step was investigated.

In the first generation flow synthesis of **4**, the compound was purified by a “catch and release” protocol using a sulfonic acid resin (QP-SA) (Scheme 6). Whilst this was effective, an excess (6 equivalents) of the immobilised acid was required to achieve complete scavenging. This is principally due to the slow diffusion of the reaction mixture into the polymer matrix and the channelling of the product solution around the spherical beads. The product (**4**) is therefore not rapidly trapped onto the resin and a concentrated band of product is not achieved. Similarly, upon release of the product a diffuse output is obtained since diffusion back out of the solid matrix must also occur. Whilst this is not normally a problem in the final step of a synthesis, the intention was to release the product directly into the next step where a concentrated slug of material would be preferred.

Alternatively, QuadraSil-SA (SS-SA), a sulfonic acid functionalised silica, exists as much smaller particles possessing a much higher functional surface area. The scavenge is much faster as the product does not need to diffuse into the particles since the functionality is present only on the silica surface. Whilst the functional loading is lower (0.8 mmol g^{-1} compared to 3.0 mmol g^{-1}), it was hoped that this enhanced surface area would provide quick and efficient scavenging of **4** followed by its equally rapid release. The flow reactor system was set up as shown in Scheme 9. The amounts of PS-NCO and *N*-methylpiperazine used were calculated based on an expected yield of 40 mg (0.118 mmol) of **9** as determined in previous experiments. The corresponding quantity of silica-supported sulfonic acid used was based on a 100% yield over both steps to ensure that all of the potential **4** formed could be theoretically captured. Following release of the product with a solution of NH_3 in MeOH (2 M), the product was isolated in 47% yield over the 2 flow steps in excellent purity ($>95\%$). This



Scheme 9 Two step integrated flow synthesis of amide **4**.

corresponds to an 80% yield for the second step, a significant improvement on the 56% obtained previously using the PS-TBD.

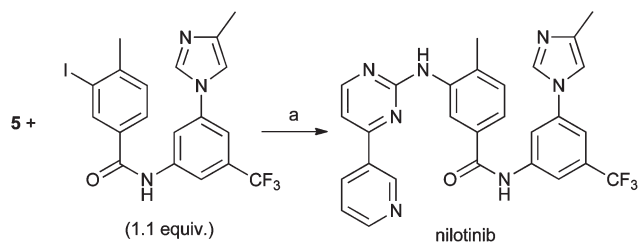
During the capture phase of the sequence, the column of silica-supported sulfonic acid underwent a visual change from translucent to opaque as the product was sequestered. This was a useful observation indicating how far the reaction had progressed. With this flow procedure in place, we investigated the crucial C–N coupling reaction.

Buchwald–Hartwig coupling of 4 and 5

Buchwald–Hartwig couplings have been previously performed in microreactors, albeit with substrates possessing good solubilities in non-polar systems.¹⁵ Traditionally, solvents such as toluene, xylene and 1,4-dioxane have been used for these reactions as they are poor ligands for Pd and do not compete with the added phosphines. Unfortunately, many of the reaction components in this work displayed poor solubility in these solvents hence the first task was to devise a more appropriate solvent system. A similar coupling strategy involving 5 had been used in a synthesis of nilotinib (Scheme 10), a second generation tyrosine kinase inhibitor that has been used to treat patients who have developed resistance to imatinib from mutations in the Bcr-Abl gene.¹⁶ This procedure employed a 2 : 1 mixture of 1,4-dioxane and *t*-BuOH. In this mixture both 4 and 5 readily dissolve on gentle heating.

We therefore used a 1,4-dioxane–*t*-BuOH mixture with a number of different bases (Table 5). The XantPhos ligand¹⁷ was used in preference to *rac*-BINAP since it had been previously shown to be effective in this and other reactions¹⁸ and results in more soluble Pd complexes.

From these results, it was clear that the choice of base used in the reaction was of great importance. The parameters described in entry 3, Table 5 resulted in 100% conversion of 4 and a 57% isolated yield of imatinib (1) after chromatography. However, these conditions are not ideal for converting to a flow process since the reaction produced solid sodium bromide and Pd black as it progressed. Performing the reaction in the presence of Cs₂CO₃ as the base was also successful, albeit the reaction was slower than with NaO*t*-Bu. Whilst the solubility of Cs₂CO₃ was poor, the solution itself remained transparent with any Pd black generated adhering to the carbonate. From the various carbonates used, only Cs₂CO₃ gave

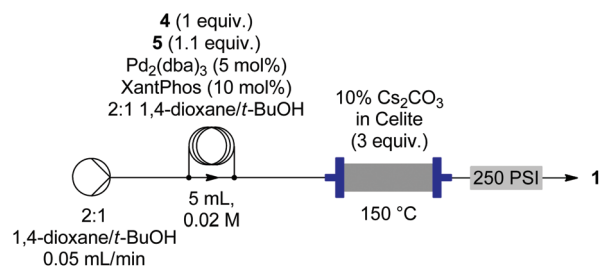


Scheme 10 Synthesis of nilotinib. Conditions: (a) Cs₂CO₃ (1.4 equiv.), Pd₂(dba)₃ (5 mol%), XantPhos (10 mol%), 2 : 1 1,4-dioxane–*t*-BuOH, 100 °C, 7 h, 89%.

Table 5 Screening of bases in the formation of 1

Entry	Base	Temperature ^a (°C)	Time (h)	Conversion ^b (%)
1	NaO <i>t</i> -Bu	100	1	40
2	NaO <i>t</i> -Bu	120	0.5	60
3	NaO <i>t</i> -Bu	150	0.5	100 (57 yield)
4	Na ₂ CO ₃	100	1	0
5	K ₂ CO ₃	100	1	0
6	KO <i>t</i> -Bu	100	1	0
7	Cs ₂ CO ₃	100	1	<10
8	Cs ₂ CO ₃	120	1	<10
9	Cs ₂ CO ₃	140	1	60
10	Cs ₂ CO ₃	150	1	70
11	Cs ₂ CO ₃	150	2	95
12	K ₃ PO ₄	150	1	0

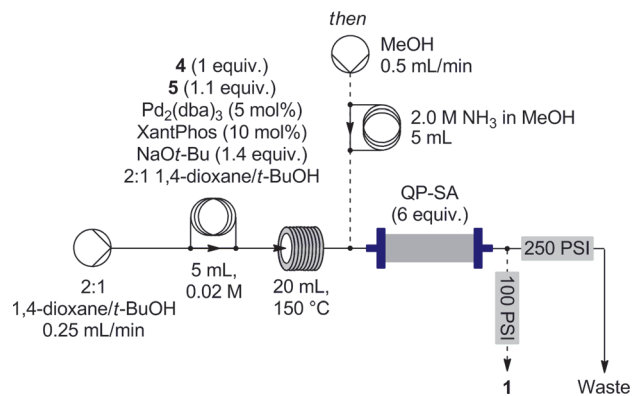
^a Heating performed by MW irradiation. ^b Conversion measured by HPLC.



Scheme 11 Attempted flow formation of 1 by Buchwald–Hartwig coupling over Cs₂CO₃.

any conversion to the product, which may be a result of its slightly higher solubility in organic solvents.¹⁹ The low solubility of Cs₂CO₃ implied that it could be packed into a column held at the desired temperature and the coupling components passed through the cartridge of reagents to react (Scheme 11).

Unfortunately, simply loading the Cs₂CO₃ directly into the column gave a very low column volume resulting in a short residence time of no more than 1 min. In order to generate the 2 h residence time required for the reaction to go to completion (entry 11, Table 5), a very large excess of Cs₂CO₃ would be required which is clearly not efficient. Alternatively, the residence time could be increased by mixing the Cs₂CO₃ with an inert packing material (in this case Celite) in order to generate a larger column packing volume. The lowest flow rate that the pump could reliably reproduce before solvent boiling occurred was 0.05 mL min⁻¹, giving a residence time of approximately 30 min resulting in only 60% conversion. Unfortunately, when this reaction was repeated it was also very unreliable. The reaction was instead repeated with a column of K₂CO₃ (1200 equivalents), a much cheaper carbonate to increase the residence time. Whilst a conversion of 50% was observed, this was almost exclusively the protodehalogenated product.



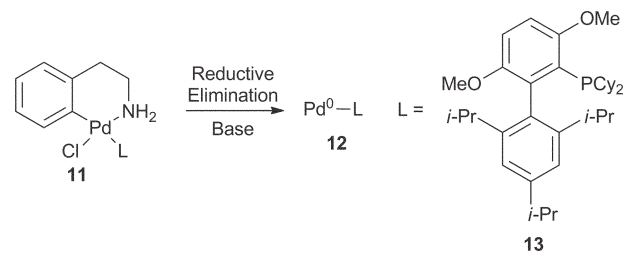
Scheme 12 Attempted flow formation of **1** using a 2 : 1 1,4-dioxane-*t*-BuOH, NaOt-Bu system.

We therefore returned to using a 2 : 1 mixture of 1,4-dioxane-*t*-BuOH with NaOt-Bu as a base despite the potential solubility issues encountered previously. In an effort to reduce the issues of solubility, the reaction concentration was reduced to 0.02 M based on amide **4**. Furthermore, a column of QP-SA was placed in-line at the end of the reactor to sequester any product generated as its salt. This material could then be released by washing the column with a solution of NH₃ in MeOH (2 M) allowing concentration of the product (Scheme 12).

During the real reaction run, a large amount of black solid was generated which accumulated at the entry to the QP-SA column thus eventually blocking the reactor. However, this blockage occurred after the solution-phase components had been trapped on the QP-SA cartridge. Consequently it was still possible to assess the reaction components following their release with NH₃/MeOH. The residue was analysed by NMR spectroscopy which indicated the reaction had not gone to completion giving a ratio of 5 : 4 : 2 4-1-protodehalogenated **4**. Increasing the concentration of the Pd catalyst to 10 mol% with 20 mol% of the ligand resulted in complete conversion, however the problem of Pd precipitation persisted.

A large number of biarylphosphane ligands are reported to be very effective in the Buchwald-Hartwig amination and by changing the substitution pattern on the ligand the catalytic process can be tailored to specific reactant combinations.²⁰ BrettPhos (**13**) is a biarylphosphane ligand recently developed by Buchwald *et al.* and has been shown to be especially active in the coupling of electron-deficient anilines with aryl mesylates and chlorides.²¹ This work has been extended by using the Pd precatalyst technology that allows *in situ* generation (Scheme 13) of an active Pd⁰ species (**12**) from an air stable Pd^{II} complex (**11**).²² It was hoped that by using this stabilised catalyst, the amount of Pd black produced in the reaction would be significantly reduced and thus result in a reaction more amenable to continuous flow processing.

This catalyst combination was therefore tested in flow (Scheme 14). In our previous reactor set-ups, the very dark colour of the Pd₂(dba)₃ catalyst in solution prevented the physical form of the components in the mixture from being



Scheme 13 BrettPhos ligand (**13**) and formation of **12** from BrettPhos Pd precatalyst **11**.

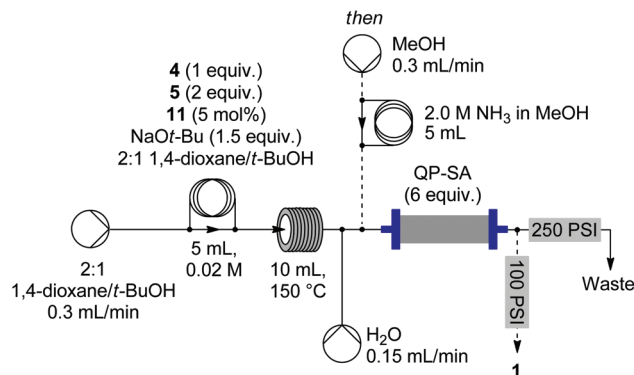
observed. In this new case, the colourless precatalyst (**11**) showed the mixture to be comprised of a very fine suspension of the catalyst. It was found that sonication of the reactant mixture did not lead to a homogeneous solution, but did fragment the larger particles allowing the mixture to be injected as a free flowing liquid. After approximately 2 min inside the reactor, small particles of solid appeared in the flow stream that continued to flow freely around the reactor coil without creating a blockage. These particles were colourless and were attributed to the NaBr generated during the reaction. The amount of black particulate generated was substantially reduced compared to the reaction using Pd₂(dba)₃/XantPhos. Since the precipitation of the NaBr during the reaction could not be avoided, a stream of water was introduced post-reactor to dissolve any inorganic solid before reaching the frit of the QP-SA column where the previous blockage had occurred.

LC-MS analysis of the reaction output indicated that no product (**1**) had passed through the cartridge of QP-SA. Following a wash of the QP-SA column with MeOH, the product was released with a solution of NH₃ in MeOH. ¹H NMR analysis of the crude output showed it to be a mixture of compounds 1-5-4-protodehalogenated **4** in the ratio 20 : 22 : 3 : 2 corresponding to a 61% theoretical yield of imatinib (**1**) based on the mass of collected material.

In-line purification of imatinib (**1**)

It was hoped that the product of the Buchwald-Hartwig coupling (Scheme 14) could be purified in-line through the use of further solid-supported reagents. However the ability to chemically differentiate between compounds **4**, the protodehalogenated derivative of **4** and the desired product **1** would be challenging. Fortunately, the primary amine functionality in **5** could act as a handle to enable selective scavenging of this component from the mixture. It was hoped that this being the case, the other impurities would be at such a low concentration as to allow purification of **1** by simple crystallisation.

A number of commercially available electrophilic scavenging agents were screened to remove **5**: Polymer-supported cyanuric chloride rapidly scavenged **5**, but could not be used since it also sequestered **1** whilst polymer-supported α -chloroacetone and acetoacetate were not effective scavengers for **5**. An attempt to selectively sequester the more basic product **1** using weak polymer-supported acids QP-IDA (QuadraPure imino diacetic acid) and QP-MPA (QuadraPure mercaptophenyl amino)



Scheme 14 Flow synthesis of imatinib using BrettPhos Pd precatalyst (**11**).

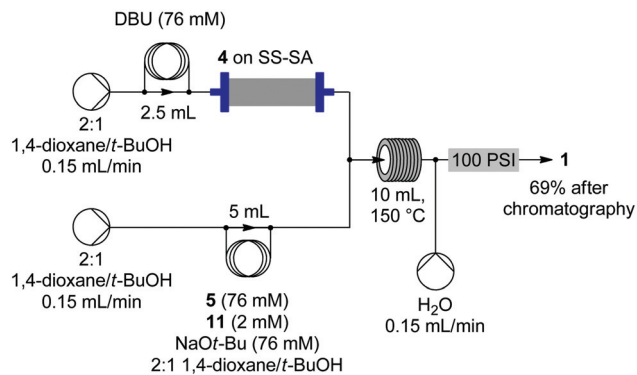
was made but both **1** and **5** were equally captured by the resins. Likewise, selective release of **5** from a mixture of **1** and **5** previously sequestered on QP-SA using pyridine as a weak base also resulted in elution of both compounds. Chromatography was therefore selected as the most timely and practical solution to the problem in preference to a “catch and release” method.

Integration with steps 1 and 2 to complete the flow synthesis

Having successfully transferred the Buchwald–Hartwig reaction to flow, the next challenge was to couple in the previous two steps by releasing **4** from the silica-supported sulfonic acid (SS-SA). It was envisaged that the captured material could be released directly into a stream containing the coupling reagents thus avoiding any manual handling of **4**. Ideally, this would have been achieved using NaO*t*-Bu as the liberating base since it was already required to perform the coupling. However, when a solution of NaO*t*-Bu in 2:1 1,4-dioxane–*t*-BuOH was pumped through the column of SS-SA, the frits containing the immobilised acid became blocked. As a result DBU was selected as a substitute base since it is a stronger base than the methylpiperazine present in **4** thereby releasing **4** quickly and efficiently. Furthermore, when an equivalent of DBU was tested in batch using similar conditions to the flow process, neither the conversion nor amount of the protodehalogenated derivative of **4** generated was affected.

For the flow set-up, two reagent streams were required since the NaO*t*-Bu caused a blockage in the silica-supported sulfonic acid column. Compound **5** could be introduced *via* either stream, but it was hoped that by injecting a 1:1.5 solution of DBU and **5** respectively into the column containing sequestered **4**, the two starting materials **4** and **5** would be eluted in the correct ratio, thus minimising the amount of **5** used. Unfortunately, this approach did not work since the UV trace of the output stream showed the presence of a chromatographic effect, thus affecting the stoichiometric ratio.

Releasing species **4** with DBU into a stream of **5**, **11** and NaO*t*-Bu was therefore the most appropriate option. A preliminary investigation indicated that DBU quantitatively and steadily released **4** from the SS-SA column over the course of 15 min. This was a key observation enabling the two reagent



Scheme 15 Release of **4** on SS-SA directly into Buchwald–Hartwig coupling.

streams to be calibrated to match. Ideally a second UV detector could be introduced at this point to automatically trigger the second stream pump.

The system was constructed as shown in Scheme 15. The column containing **4** sequestered on SS-SA from the previous step (Scheme 9) with an assumed content of 38 mg of **4** was installed into the system. Following priming of the column with 2:1 1,4-dioxane–*t*-BuOH, a solution of DBU was injected into the column to release **4**. After 10 min, a second stream containing the Buchwald coupling components was injected to meet the released stream of **4** at a T-piece mixer. The injection of the solution of coupling reagents was timed such that the slug reached the T-piece ~5 min before the solution of **4** to ensure a stable concentration was maintained and to take into account any variation in the release time of **4**.

Following evaporation of the solvent from the output stream, the residue was purified by column chromatography on silica to give imatinib in 69% yield or 32% over the 3 step procedure. Whilst the yield is lower than that described in the literature,²³ the ability to produce imatinib in a single procedure with only one manual purification step is a significant advantage especially for analogue generation.

Analogue synthesis

Having established a workable flow procedure to imatinib, we next focused on applying the approach to the preparation of various analogues (Fig. 8). The route permits significant variation of the R''' substituent which is not readily achievable with the methods used in the normal process route.⁷ Variation of –NR'R'' is also possible, however the nitrogen must remain basic enough to allow the product to be captured on the SS-SA resin for purification. Whilst the substitution patterns of the rest of the structure could be varied, the core structure was preserved throughout the compound library.

Dispersion issues during analogue formation

Initially the formation of compound **21** (R=F) was attempted using identical conditions to those used in the successful synthesis of imatinib (**1**). However, the dispersion obtained when the 3-bromo-4-fluoroaniline was passed through the column containing the PS-DMAP activated acyl chloride was

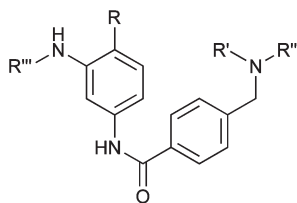


Fig. 8 Scope of analogue formation.

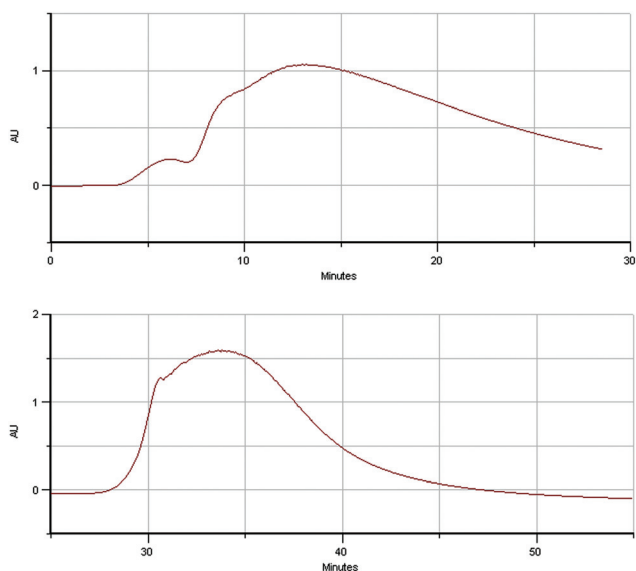


Fig. 9 Dispersion observed during amide formation during the synthesis of **21**. Top: using PS-DMAP. Bottom: solution phase. (UV recorded at 340 nm.)

significantly greater (Fig. 9, top). The distinct shoulders seen in the UV trace arose from aniline impurities which caused problems with the fraction collection that could not easily be overcome. Alternatively, the solution phase method (Scheme 5), in which a stream of acid chloride **8** and DIPEA is mixed with a stream of the aniline, was successful, but was not used previously in the 2-step coupling sequence as the dispersion was too great. However, with the development of the in-line solvent switching technique, this dispersion effect was no longer such an important issue since the solvent is removed. It was also found that the addition of a small plug of silica at the end of the column scavenged any residual DIPEA salts and as a result the quantity of polymer-supported scavengers could be reduced thus minimising product dispersion. Furthermore, the silica also trapped the coloured impurities present in the aniline starting material (Fig. 10) pleasingly resulting in a product of even greater purity. Consequently, this general method was subsequently applied in the synthesis of all further analogues (Scheme 16). The UV trace (Fig. 9, bottom) of the output stream displays a much improved peak profile as compared to that observed using PS-DMAP (Fig. 9, top).

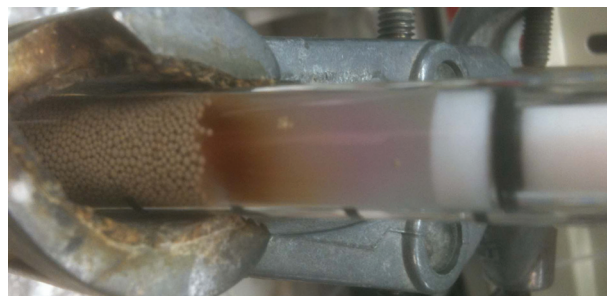


Fig. 10 Aniline impurities trapped on silica plug.

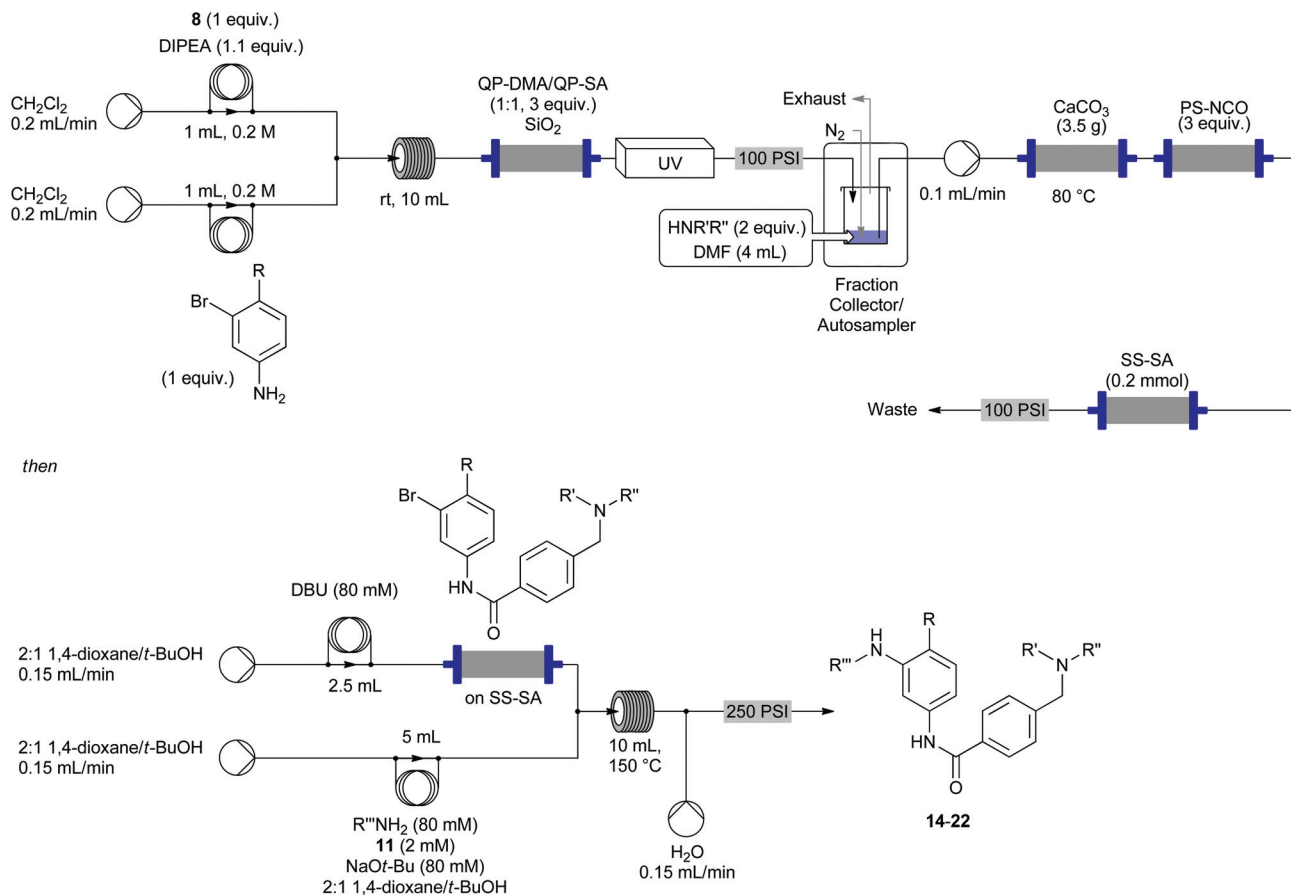
Analogue synthesis using the final flow reactor set-up

A number of analogues were prepared (Table 6) using the reactor shown in Scheme 16. The structures were designed to mimic the pharmacophores present in the original imatinib structure. Compound **24** was chosen as a starting material since it could potentially be made in flow.²⁴ Each analogue was formed in a single procedure and the stoichiometries of the reagents used in the benzyl chloride substitution were based on an 80% estimated yield for the amide formation. The amount of SS-SA was used such that all of the product could be captured effectively. The concentration ratios of the Buchwald coupling were identical to those previously used, however the amount of DBU used was increased to match the functional loading of the SS-SA column.

Only the reaction with imidazole (Table 6, entry 7) did not yield any of the desired product as the intermediate generated was not effectively sequestered by the acidic column. In addition, the formation of the imidazole-substituted intermediate only proceeded in low conversion, presumably as a result of the reduced nucleophilicity of the imidazole.

Whilst purification of imatinib (**1**) by column chromatography (SiO₂) worked well using MeOH as the mobile phase, this method was not always effective for purification of the analogues. A CH₂Cl₂/MeOH/NH₃ system proved effective, but a more efficient separation was observed if the chromatography was performed after an aqueous work-up to remove the salts produced during the reaction.

The analogues produced were submitted to Pfizer Ltd. for screening against Abl1 and the % inhibition values obtained are shown in Table 6 along with imatinib itself. The methyl group *ortho* to the aminopyrimidine substituent is known to be important to the activity of **1**. This was reflected in the present study since replacement of the methyl group with a fluoro (Table 6, entry 9) or trifluoromethoxy (Table 6, entry 10) group substantially reduced the inhibition of Abl1. Changes to the piperazine moiety (compounds **18**, **19** and **20**) also showed a reduction in activity, albeit not to the same extent as alterations elsewhere. This illustrates that the piperazine is important to receptor binding rather than simply functioning as a solubilising group. Modifications to the aminopyrimidine portion of the molecule (–NR''') were less tolerated and only compound **14** displayed any significant activity. This may be due to the nitrogen in the benzimidazole substituent being



Scheme 16 Reactor set-up for the synthesis of analogues 14–22.

positioned in a similar location and orientation to that of the pyridyl substituent in **1**.

Conclusions

A flow process has been developed that leads to the preparation of imatinib without the need for any manual handling of intermediates over a three step process. The synthesis was achieved despite the poor solubility of individual components and methods were developed to overcome these. In addition the use of an in-line solvent switching technique permitted reaction solvents to be changed as part of the continuous process and this could be used for a number of different applications. Using this method enables imatinib to be synthesised in high purity in less than a day. The generic reactor set-up was then utilised to prepare a number of analogues in similar yield that were not directly obtainable using the original process route described.

Further work to fully automate the flow reactor and couple it with an in-line purification, quantification and even a screening device would enable an imatinib analogue to be synthesised and screened in a single process.

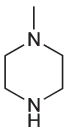
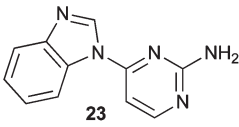
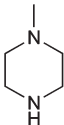
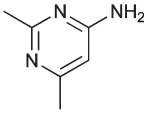
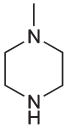
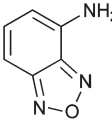
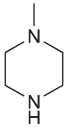
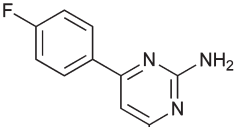
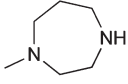
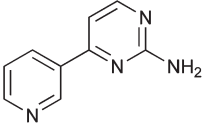
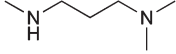
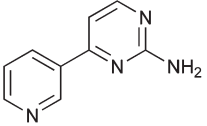
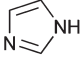
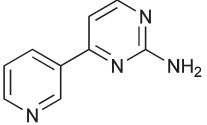
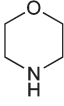
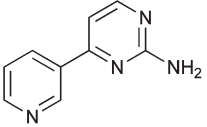
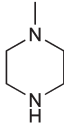
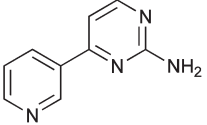
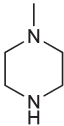
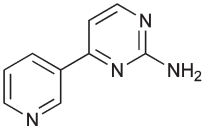
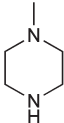
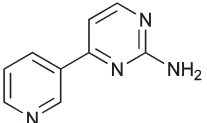
Experimental

Experimental details are provided for the flow synthesis of imatinib (**1**) and compounds 14–22. For the synthesis of intermediates, please refer to the ESI.†

General

¹H NMR spectra were recorded on a Bruker Avance DPX-400, DRX-500 or DRX-600 spectrometer with residual CHCl₃, CD₂HOD or DMSO as the internal reference. ¹³C NMR spectra were recorded on the same spectrometers with the central peak of CDCl₃, CD₃OD or d₆-DMSO as the internal reference. Infrared spectra were recorded as a neat thin film on a Perkin-Elmer Spectrum One FT-IR spectrometer using Universal ATR sampling accessories. Melting points were obtained using an OptiMelt automated melting point system available from Stanford Research Systems calibrated against vanillin (mp 83 °C), phenacetin (mp 136 °C) and caffeine (mp 237 °C). High resolution mass spectrometry (HRMS) was carried out on a Waters Micromass LCT Premier spectrometer using time of flight with positive and negative electrospray ionisation. LC-MS analysis was performed with an Agilent HP 1100 series chromatograph (Mercury Luna 3μ C18 (2) column) attached to a Waters ZQ2000 mass spectrometer with ESCi ionisation

Table 6 Synthesis of analogues **14–22** using the flow reactor (Scheme 16)

Entry	R	HNR'R''	R'''NH ₂ ^a	Product	Isolated yield ^b (%)	% Inhibition ^e
1	Me		 23	14	27	75.0
2	Me			15	33	5.0
3	Me			16	31	16.5
4	Me		 24	17	26	4.0
5	Me			18	25 ^c	38.5
6	Me			19	24 ^c	47.0
7	Me			—	—	—
8	Me			20	24	30.0
9	F			21	35	9.0
10	OCF ₃			22	28	4.5
11	Me			1	32 ^d	88.0

^a Compounds **23** and **24** were synthesised in batch from commercially available starting materials. ^b Isolated yields after column chromatography. ^c Purified by preparative TLC. ^d Yield from reactor using catch and release amide formation. ^e % inhibition of Abl1 at ATP Km using 1 μM concentration of compound.

source in ESI mode. Elution was carried out at a flow rate of 0.6 mL min^{-1} using a reverse phase gradient of MeCN and H_2O containing 0.1% formic acid using a gradient with the following proportions of MeCN (0 min, 5%; 1 min, 5%, 4 min, 95%; 5 min, 95%; 7 min, 5%; 8 min, 5%). Rt is the retention time in minutes and the m/z value is reported. Unless otherwise specified, reagents were obtained from commercial sources and used without further purification. The conc. NH_3 (aq) used was 18 M concentration. The PE used refers to the fraction boiling in the range 40–60 °C. Laboratory reagent grade solvents CH_2Cl_2 , EtOAc, *n*-hexane, and PE were obtained from Fischer Scientific and distilled before use. Dry CH_2Cl_2 was obtained by distillation over CaH_2 . THF was obtained from Fischer Scientific and distilled over LiAlH_4 and CaH_2 with triphenylmethane as an indicator. TLC was performed on Merck 60 F254 silica gel plates and were visualised using short-wave ultra-violet light. Flash column chromatography was performed using silica gel (0.040–0.063 mm), purchased from Breckland Scientific Supplies. Preparative TLC was conducted using $20 \times 20 \text{ cm}$ Merck 60 F254 silica gel plates.

All columns of polymer-supported reagents were pre-conditioned with the reaction solvent before use and the plunger inserted to the resultant swelled height of the resin. Sources of equipment: Vapourtec R2+/R4 flow system: Vapourtec Ltd. (website: <http://www.vapourtec.com>). Gilson equipment and Unipoint (version 5.11) software: Gilson Inc. (website: <http://www.gilson.com>). Knauer K100 pump: Wissenschaftliche Gerätebau Dr. Ing. Herbert Knauer GmbH (website: <http://www.knauer.net>). Omnifit columns: Diba Industries Ltd. (website: <http://www.omnifit.com>).

***N*-(4-Methyl-3-((4-(pyridin-3-yl)pyrimidin-2-yl)amino)phenyl)-4-((4-methylpiperazin-1-yl)methyl)benzamide 1.**⁶ Using a Knauer K100 pump, the column of SS-SA containing sequestered **4** (38 mg, 0.094 mmol) from the flow synthesis of **4** was washed with 1,4-dioxane-*t*-BuOH (2 : 1, 0.4 mL min^{-1} , 15 min). A solution (2.5 mL) of DBU (28 μL , 0.189 mmol) in 1,4-dioxane-*t*-BuOH (2 : 1) was loaded into a 5 mL sample loop and injected into the stream of 1,4-dioxane-*t*-BuOH (2 : 1) flowing through the column of SS-SA at 0.15 mL min^{-1} . A second solution (5 mL) of **5** (65 mg, 0.378 mmol), NaOt-Bu (36 mg, 0.378 mmol) and **11** (7.5 mg, $9.4 \mu\text{mol}$) in 1,4-dioxane-*t*-BuOH (2 : 1) was sonicated (10 min) and loaded into a 5 mL sample loop. This was injected into a stream of 1,4-dioxane-*t*-BuOH (2 : 1, pumped at 0.15 mL min^{-1} by a second Knauer K100 pump) 10 min after the injection of the DBU solution. The two streams were combined in a T-piece after the column of SS-SA and directed into a flow coil (10 mL) heated to 150 °C using a Vapourtec R4 heater. A stream of water (0.15 mL min^{-1}) was introduced to the output of the flow coil *via* a T-piece, the resultant stream passed through a 250 psi BPR and the output collected. The solvent was removed *in vacuo*, the residue loaded onto a Biotage silica sample with MeOH (5 mL) and purified using a Biotage SP1 chromatographic purification system¹³ (25 g SNAP cartridge) eluting with MeOH. The desired fractions were combined and the solvent removed *in vacuo*. The residue was dissolved in CH_2Cl_2 (10 mL), filtered

and the solvent removed *in vacuo* to give the title compound (32 mg, 69%) as an off-white powder; mp 206–207 °C (lit.²⁵ 207–210 °C). Rt 3.48, $[\text{M} + \text{H}]^+$ $m/z = 494.2$. R_f 0.09 (MeOH). $^1\text{H NMR}$ (600 MHz, d_6 -DMSO): $\delta/\text{ppm} = 10.14$ (1 H, s), 9.26 (1 H, d, $J = 1.5 \text{ Hz}$), 8.95 (1 H, s), 8.66 (1 H, dd, $J = 4.8$ and 1.2 Hz), 8.49 (1 H, d, $J = 5.1 \text{ Hz}$), 8.46 (1 H, ddd, $J = 7.9$, 1.5 and 1.2 Hz), 8.06 (1 H, d, $J = 1.5 \text{ Hz}$), 7.89 (2 H, d, $J = 8.1 \text{ Hz}$), 7.50 (1 H, dd, $J = 7.9$ and 4.8 Hz), 7.46 (1 H, dd, $J = 8.3$ and 1.5 Hz), 7.42–7.40 (3 H, m), 7.18 (1 H, d, $J = 8.3 \text{ Hz}$), 3.51 (2 H, s), 2.30 (8 H, br s), 2.20 (3 H, s), 2.13 (3 H, s). $^{13}\text{C NMR}$ (150 MHz, CDCl_3): $\delta/\text{ppm} = 165.42$ (C), 162.72 (C), 160.57 (C), 158.99 (CH), 151.44 (CH), 148.48 (CH), 142.52 (C), 137.77 (C), 136.60 (C), 134.92 (CH), 133.88 (C), 132.66 (C), 130.75 (CH), 129.28 (CH), 127.00 (CH), 124.23 (C), 123.71 (CH), 115.35 (CH), 113.19 (CH), 108.32 (CH), 62.49 (CH_2), 55.07 (CH_2), 53.10 (CH_2), 45.98 (CH_3), 17.65 (CH_3). IR: $\nu_{\text{max}} = 3275\text{w}$, 2929w, 2797w, 1646m, 1586m, 1575s, 1554m, 1532s, 1510m cm^{-1} . HRMS calculated for $\text{C}_{29}\text{H}_{31}\text{N}_7\text{O}_2\text{Na}$, $[\text{M} + \text{Na}]^+$, 516.2488; found 516.2491, $\Delta = 0.8 \text{ ppm}$.

General procedure for the flow preparation of 14–22

Using a Vapourtec R2+, a solution of an aniline (0.20 mmol) in dry CH_2Cl_2 (1 mL) was loaded into a 1 mL injection loop. A solution of 4-(chloromethyl)benzoyl chloride (0.20 mmol) and DIPEA (38 μL , 0.22 mmol) in dry CH_2Cl_2 (1 mL) was loaded into a second sample loop. The sample loops were switched in-line with streams of dry CH_2Cl_2 (0.2 mL min^{-1} each) simultaneously, mixed in a T-piece and the mixed stream flowed into a 10 mL coil of tubing held at rt. The output was then directed into a 6.6 mm Omnifit column filled with sequential layers of QP-DMA (200 mg, 0.6 mmol), QP-SA (200 mg, 0.6 mmol) and SiO_2 (350 mg). The stream was then directed through a Gilson 170 UV DAD (340 nm monitor, 550 nm reference), a 100 psi BPR then into a Gilson 233XL fraction collector/autosampler. The UV detector and fraction collector were controlled by Gilson Unipoint software. The fraction collector was set to collect the output of the reaction when the UV absorption was over 7.5% of the full scale into a tapered 20 mL vial with a screw-top septum containing a solution (4 mL) of an amine (0.32 mmol) in DMF. A PTFE tube connected to a nitrogen gas supply (0.5 bar) bubbled nitrogen through the solution during collection, with a second polymer tube placed at the top of the vial to allow solvent vapours to vent to an exhaust. The vial was placed on a hotplate set to 65 °C to provide a solution temperature of approximately 50 °C. When the collection was complete, the solution was allowed to stand with nitrogen bubbling through the solution for a further 30 min (50 °C). Using Gilson Unipoint software, the injector was set to aspirate air (100 μL), followed by the reaction solution (5 mL) into a sample loop (20 mL) using a Gilson 402 syringe pump. This was injected into a sample loop (10 mL) and switched in-line with a switching valve into a stream of DMF flowing at 0.1 mL min^{-1} . The flow stream was then directed into a 10 mm diameter Omnifit column packed with CaCO_3 (3.5 g, 35 mmol) and a layer of SiO_2 (300 mg) and a further 6.6 mm diameter Omnifit column packed with PS-NCO

(369 mg, 0.48 mmol). The output of this column was directed through a 3.0 mm diameter Omnifit column packed with SS-SA (250 mg, 0.20 mmol) and then a 100 psi BPR before directing the output to waste. After 1.5 h, the column was washed with 1,4-dioxane-*t*-BuOH (2 : 1, 0.4 mL min⁻¹, 15 min) using a Knauer K100 pump. A solution (2.5 mL) of DBU (30 μL, 0.20 mmol) in 1,4-dioxane-*t*-BuOH (2 : 1) was loaded into a 5 mL sample loop and injected into the stream of 1,4-dioxane-*t*-BuOH (2 : 1) flowing through the column of SS-SA at 0.15 mL min⁻¹. A second solution (5 mL) of an aryl amine (0.40 mmol), NaOt-Bu (38 mg, 0.40 mmol) and **11** (8 mg, 10 μmol) in 1,4-dioxane-*t*-BuOH (2 : 1) was sonicated (10 min) and loaded into a 5 mL sample loop. This was injected into a stream of 1,4-dioxane-*t*-BuOH (2 : 1, pumped at 0.15 mL min⁻¹ by a second Knauer K100 pump) 10 min after the injection of the DBU solution. The two streams were combined in a T-piece after the column of SS-SA and directed into a flow coil (10 mL) heated to 150 °C using a Vapourtec R4 heater. A stream of water (0.15 mL min⁻¹) was introduced to the output of the flow coil *via* a T-piece, the resultant stream passed through a 250 psi BPR and the output collected. The solution was then concentrated *in vacuo* and the residue partitioned between CH₂Cl₂ (25 mL) and water (25 mL). The aqueous layer was extracted with further CH₂Cl₂ (3 × 10 mL), the organic layers combined and washed with water (30 mL), brine (30 mL) and dried (Na₂SO₄). The solvent was removed *in vacuo* and the residue purified by chromatography with the specified solvent system.

N-(3-((4-(1*H*-Benzo[*d*]imidazol-1-yl)pyrimidin-2-yl)amino)-4-methylphenyl)-4-((4-methylpiperazin-1-yl)methyl)benzamide **14**. Purified by column chromatography (94 : 5 : 1 CH₂Cl₂-MeOH-conc. NH₃(aq)) to give the title compound (29 mg, 27%, >95% purity) as an off-white powder; mp 204–207 °C. Rt 3.62, [M + H]⁺ *m/z* = 533.3. *R*_f 0.28 (94 : 5 : 1 CH₂Cl₂-MeOH-conc. NH₃(aq)). ¹H NMR (600 MHz, CDCl₃): δ/ppm = 8.65 (1 H, s), 8.47 (1 H, d, *J* = 5.2 Hz), 8.32 (1 H, s), 8.10 (1 H, s), 8.05 (1 H, m), 7.79–7.75 (3 H, m), 7.49 (1 H, d, *J* = 8.0 Hz), 7.37 (2 H, d, *J* = 7.9 Hz), 7.27–7.25 (2 H, m), 7.23 (1 H, d, *J* = 8.0 Hz), 7.19 (1 H, s), 6.91 (1 H, d, *J* = 5.2 Hz), 3.53 (2 H, s), 2.51 (8 H, br s), 2.33 (3 H, s), 2.32 (3 H, s). ¹³C NMR (150 MHz, CDCl₃): δ/ppm = 165.55 (C), 160.65 (C), 160.32 (CH), 156.65 (C), 144.88 (C), 142.62 (C), 140.98 (CH), 137.04 (C), 136.72 (C), 133.62 (C), 131.60 (C), 130.97 (CH), 129.93 (CH), 127.04 (CH), 125.62 (C), 124.65 (CH), 123.89 (CH), 120.78 (CH), 116.39 (CH), 114.57 (CH), 114.26 (CH), 100.13 (CH), 62.48 (CH₂), 55.09 (CH₂), 53.12 (CH₂), 46.02 (CH₃), 17.60 (CH₃). IR: ν_{max} = 3203w, 2931w, 2794w, 1664w, 1593m, 1568m, 1528m cm⁻¹. HRMS calculated for C₃₁H₃₃N₈O, [M + H]⁺, 533.2777; found 533.2792, Δ = 2.8 ppm.

N-(3-((2,6-Dimethylpyrimidin-4-yl)amino)-4-methylphenyl)-4-((4-methylpiperazin-1-yl)methyl)benzamide **15**. Purified by column chromatography (94 : 5 : 1 CH₂Cl₂-MeOH-conc. NH₃(aq)) to give the title compound (29 mg, 33%) as an off-white powder; mp 170–174 °C dec. Rt 3.08, [M + H]⁺ *m/z* = 445.3. *R*_f 0.22 (94 : 5 : 1 CH₂Cl₂-MeOH-conc. NH₃(aq)). ¹H NMR (600 MHz, CDCl₃): δ/ppm = 8.13 (1 H, s), 7.80 (2 H, d, *J* = 8.0

Hz), 7.68 (1 H, d, *J* = 1.5 Hz), 7.41 (3 H, m), 7.23 (1 H, d, *J* = 8.2 Hz), 6.79 (1 H, s), 6.18 (1 H, s), 3.54 (2 H, s), 2.47 (3 H, s), 2.46 (8 H, br s), 2.29 (3 H, s), 2.27 (3 H, s), 2.21 (3 H, s). ¹³C NMR (125 MHz, CDCl₃): δ/ppm = 167.40 (C), 166.49 (C), 165.49 (C), 161.63 (C), 142.51 (C), 136.72 (C), 136.66 (C), 133.61 (C), 131.52 (CH), 129.36 (CH), 128.96 (C), 127.03 (CH), 117.86 (CH), 116.86 (CH), 99.22 (CH), 62.26 (CH₂), 54.83 (CH₂), 52.45 (CH₂), 45.56 (CH₃), 25.80 (CH₃), 24.20 (CH₃), 17.47 (CH₃). IR: ν_{max} = 3196w, 2939w, 2798w, 1649w, 1586s, 1527m, 1505m cm⁻¹. HRMS calculated for C₂₆H₃₃N₆O, [M + H]⁺, 445.2716; found 445.2729, Δ = 2.9 ppm.

N-(3-(Benzo[*c*][1,2,5]oxadiazol-4-ylamino)-4-methylphenyl)-4-((4-methylpiperazin-1-yl)methyl)benzamide **16**. Purified by column chromatography (85 : 15 CH₂Cl₂-MeOH) to give the title compound (28 mg, 31%) as a bright orange solid; mp 113–117 °C. Rt 4.00, [M + H]⁺ *m/z* = 457.3. *R*_f 0.31 (85 : 15 CH₂Cl₂-MeOH). ¹H NMR (600 MHz, CDCl₃): δ/ppm = 7.94 (1 H, s), 7.91 (1 H, s), 7.80 (2 H, d, *J* = 8.1 Hz), 7.43 (2 H, d, *J* = 8.1 Hz), 7.26–7.23 (3 H, m), 7.15 (1 H, d, *J* = 8.9 Hz), 6.59 (1 H, d, *J* = 7.2 Hz), 6.53 (1 H, s), 3.55 (2 H, s), 2.47 (8 H, br s), 2.29 (6 H, s). ¹³C NMR (150 MHz, CDCl₃): δ/ppm = 165.63 (C), 150.06 (C), 145.27 (C), 142.84 (C), 138.07 (C), 136.85 (C), 133.82 (CH), 133.49 (C), 133.02 (C), 131.57 (CH), 129.35 (CH), 127.47 (C), 126.98 (CH), 116.65 (CH), 114.94 (CH), 104.84 (CH), 104.36 (CH), 62.46 (CH₂), 55.07 (CH₂), 53.08 (CH₂), 45.99 (CH₃), 17.32 (CH₃). IR: ν_{max} = 3295w, 2935w, 2801w, 1650m, 1599m, 1561s, 1528s, 1508m cm⁻¹. HRMS calculated for C₂₆H₂₉N₆O₂, [M + H]⁺, 457.2352; found 457.2363, Δ = 2.4 ppm.

N-(3-((4-(4-Fluorophenyl)-6-phenylpyrimidin-2-yl)amino)-4-methylphenyl)-4-((4-methylpiperazin-1-yl)methyl)benzamide **17**. Purified by column chromatography (9 : 1 CH₂Cl₂-MeOH) to give the title compound (30 mg, 26%) as a pale yellow powder; mp 228–231 °C dec. Rt 4.35, [M + H]⁺ *m/z* = 587.3. *R*_f 0.28 (9 : 1 CH₂Cl₂-MeOH). ¹H NMR (600 MHz, CDCl₃): δ/ppm = 8.87 (1 H, d, *J* = 1.5 Hz), 8.21 (2 H, dd, *J* = 8.6 and 5.4 Hz), 8.17–8.16 (2 H, m), 7.85 (1 H, s), 7.84 (2 H, d, *J* = 8.0 Hz), 7.54 (1 H, s), 7.51–7.50 (3 H, m), 7.45 (2 H, d, *J* = 8.0 Hz), 7.25 (1 H, dd, *J* = 8.2 and 1.5 Hz), 7.19–7.15 (3 H, m), 7.09 (1 H, s), 3.58 (2 H, s), 2.53 (8 H, br s), 2.37 (3 H, s), 2.33 (3 H, s). ¹³C NMR (150 MHz, CDCl₃): δ/ppm = 165.96 (C), 165.14 (C), 164.69 (C), 164.46 (C, d, *J* = 250.6 Hz), 160.52 (C), 142.42 (C), 138.40 (C), 137.48 (C), 136.51 (C), 133.98 (C), 133.65 (C, d, *J* = 3.2 Hz), 130.67 (CH), 130.58 (CH), 129.41 (CH, d, *J* = 8.5 Hz), 129.31 (CH), 128.79 (CH), 127.27 (CH), 126.95 (CH), 123.26 (C), 115.75 (CH, d, *J* = 22 Hz), 114.41 (CH), 112.52 (CH), 104.36 (CH), 62.43 (CH₂), 54.99 (CH₂), 52.86 (CH₂), 45.81 (CH₃), 17.72 (CH₃). IR: ν_{max} = 3454w, 3437w, 3299w, 2933w, 2794w, 1645m, 1600m, 1588m, 1575m, 1531s, 1511m cm⁻¹. HRMS calculated for C₃₆H₃₆FN₆O, [M + H]⁺, 587.2935; found 587.2937, Δ = 0.3 ppm.

4-((4-Methyl-1,4-diazepan-1-yl)methyl)-N-(4-methyl-3-((4-pyridin-3-yl)pyrimidin-2-yl)amino)phenyl)benzamide **18**.²⁶ Purified by preparative TLC (89 : 10 : 1 CH₂Cl₂-MeOH-conc. NH₃(aq)) to give the title compound (25 mg, 25%) as an off-white solid; mp 155–160 °C dec. Rt 3.43, [M + H]⁺ *m/z* = 508.3. *R*_f 0.17 (94 : 5 : 1 CH₂Cl₂-MeOH-conc. NH₃(aq)). ¹H NMR (600 MHz,

CDCl₃): δ /ppm = 9.23 (1 H, d, J = 1.8 Hz), 8.70 (1 H, dd, J = 4.8 and 1.5 Hz), 8.58 (1 H, d, J = 1.5 Hz), 8.52–8.50 (2 H, m), 7.93 (1 H, s), 7.83 (2 H, d, J = 8.0 Hz), 7.46 (2 H, d, J = 8.0 Hz), 7.41 (1 H, dd, J = 7.8 and 4.8 Hz), 7.31 (1 H, dd, J = 8.2 and 1.5 Hz), 7.20 (1 H, d, J = 8.2 Hz), 7.17 (1 H, d, J = 5.2 Hz), 7.04 (1 H, s), 3.69 (2 H, s), 2.73–2.69 (4 H, m), 2.68 (2 H, t, J = 5.8 Hz), 2.62 (2 H, m), 2.37 (3 H, s), 2.34 (3 H, s), 1.82 (2 H, app quintet, J = 5.8 Hz). ¹³C NMR (150 MHz, CDCl₃): δ /ppm = 165.45 (C), 162.73 (C), 160.58 (C), 159.01 (CH), 151.47 (CH), 148.50 (CH), 143.97 (C), 137.78 (C), 136.62 (C), 134.92 (CH), 133.71 (C), 132.67 (C), 130.76 (CH), 128.97 (CH), 126.97 (CH), 124.17 (C), 123.71 (CH), 115.30 (CH), 113.13 (CH), 108.33 (CH), 62.45 (CH₂), 58.17 (CH₂), 56.76 (CH₂), 54.72 (CH₂), 54.34 (CH₂), 47.04 (CH₃), 27.54 (CH₂), 17.65 (CH₃). IR: ν_{\max} = 3235w, 3032w, 2929w, 2800w, 1652m, 1575s, 1553s, 1526s, 1504s cm⁻¹. HRMS calculated for C₃₀H₃₄N₇O, [M + H]⁺, 508.2825; found 508.2837, Δ = 2.4 ppm.

4-((3-(Dimethylamino)propyl)(methyl)amino)methyl)-N-(4-methyl-3-((4-(pyridin-3-yl)pyrimidin-2-yl)amino)phenyl)benzamide 19. Purified by preparative TLC (89 : 10 : 1 CH₂Cl₂-MeOH-conc. NH_{3(aq)}) to give the title compound (24 mg, 24%) as an off-white solid; mp 152–155 °C dec. Rt 3.46, [M + H]⁺ m/z = 510.3. R_f 0.16 (94 : 5 : 1 CH₂Cl₂-MeOH-conc. NH_{3(aq)}). ¹H NMR (600 MHz, CDCl₃): δ /ppm = 9.24 (1 H, d, J = 1.8 Hz), 8.70 (1 H, dd, J = 4.8 and 1.5 Hz), 8.58 (1 H, d, J = 1.5 Hz), 8.53–8.50 (2 H, m), 7.92 (1 H, s), 7.83 (2 H, d, J = 8.0 Hz), 7.44–7.40 (3 H, m), 7.31 (1 H, dd, J = 8.2 and 1.5 Hz), 7.20 (1 H, d, J = 8.2 Hz), 7.18 (1 H, d, J = 5.1 Hz), 7.04 (1 H, s), 3.54 (2 H, s), 2.41 (2 H, t, J = 7.4 Hz), 2.34 (3 H, s), 2.31 (2 H, t, J = 7.4 Hz), 2.23 (6 H, s), 2.20 (3 H, s), 1.70 (2 H, app quintet, J = 7.4 Hz). ¹³C NMR (150 MHz, CDCl₃): δ /ppm = 165.43 (C), 162.75 (C), 160.58 (C), 159.01 (CH), 151.47 (CH), 148.49 (CH), 143.59 (C), 137.78 (C), 136.61 (C), 134.94 (CH), 133.75 (C), 132.68 (C), 130.76 (CH), 129.15 (CH), 126.97 (CH), 124.18 (C), 123.72 (CH), 115.30 (CH), 113.13 (CH), 108.34 (CH), 61.98 (CH₂), 57.78 (CH₂), 55.63 (CH₂), 45.49 (CH₃), 42.26 (CH₃), 25.67 (CH₂), 17.65 (CH₃). IR: ν_{\max} = 3215w, 2940w, 2767w, 1655w, 1575s, 1526s, 1504s cm⁻¹. HRMS calculated for C₃₀H₃₆N₇O, [M + H]⁺, 510.2981; found 510.2998, Δ = 3.3 ppm.

N-(4-Methyl-3-((4-(pyridin-3-yl)pyrimidin-2-yl)amino)phenyl)-4-(morpholinomethyl)benzamide 20.²⁷ Purified by column chromatography (94 : 5 : 1 CH₂Cl₂-MeOH-conc. NH_{3(aq)}) to give the title compound (23 mg, 24%) as an off-white solid; mp 213–216 °C (lit.²⁵ 210–212 °C). Rt 3.61, [M + H]⁺ m/z = 481.2. R_f 0.29 (94 : 5 : 1 CH₂Cl₂-MeOH-conc. NH_{3(aq)}). ¹H NMR (500 MHz, CDCl₃): δ /ppm = 9.24 (1 H, d, J = 1.8 Hz), 8.70 (1 H, dd, J = 4.8 and 1.5 Hz), 8.59 (1 H, d, J = 1.6 Hz), 8.52–8.50 (2 H, m), 7.90 (1 H, s), 7.84 (2 H, d, J = 8.0 Hz), 7.45 (2 H, d, J = 8.0 Hz), 7.42 (1 H, dd, J = 7.9 and 4.8 Hz), 7.31 (1 H, dd, J = 8.2 and 1.6 Hz), 7.21 (1 H, d, J = 8.2 Hz), 7.18 (1 H, d, J = 5.2 Hz), 7.04 (1 H, s), 3.72 (4 H, t, J = 4.3 Hz), 3.56 (2 H, s), 2.46 (4 H, app br s), 2.35 (3 H, s). ¹³C NMR (150 MHz, CDCl₃): δ /ppm = 165.31 (C), 162.76 (C), 160.57 (C), 159.01 (CH), 151.49 (CH), 148.52 (CH), 141.90 (C), 137.81 (C), 136.57 (C), 134.91 (CH), 134.05 (C), 132.66 (C), 130.78 (CH), 129.34 (CH), 127.04 (CH), 124.20 (C), 123.70 (CH), 115.26 (CH), 113.07 (CH), 108.36

(CH), 66.94 (CH₂), 62.91 (CH₂), 53.62 (CH₂), 17.65 (CH₃). IR: ν_{\max} = 3230w, 2932w, 2810w, 1663m, 1606m, 1580s, 1561s, 1526s cm⁻¹. HRMS calculated for C₂₈H₂₉N₆O₂, [M + H]⁺, 481.2352; found 481.2371, Δ = 3.9 ppm.

N-(4-Fluoro-3-((4-(pyridin-3-yl)pyrimidin-2-yl)amino)phenyl)-4-((4-methylpiperazin-1-yl)methyl)benzamide 21.²⁶ Purified by column chromatography (MeOH). The fractions corresponding to the product were combined and the solvent removed *in vacuo*. The residue was dissolved in CH₂Cl₂ (5 mL), filtered and the solvent removed *in vacuo* to give the title compound (35 mg, 35%) as an off-white solid; mp 186–189 °C. Rt 3.40, [M + H]⁺ m/z = 498.3. R_f 0.11 (MeOH). ¹H NMR (500 MHz, CDCl₃): δ /ppm = 9.24 (1 H, d, J = 1.8 Hz), 8.96 (1 H, dd, J = 7.1 and 2.1 Hz), 8.70 (1 H, dd, J = 4.8 and 1.6 Hz), 8.60–8.58 (1 H, m), 8.54 (1 H, d, J = 5.2 Hz), 7.88 (1 H, s), 7.83 (2 H, d, J = 8.2 Hz), 7.47–7.42 (4 H, m), 7.29–7.26 (2 H, m), 7.09 (1 H, dd, J = 10.7 and 8.8 Hz), 3.57 (2 H, s), 2.53 (8 H, br s), 2.34 (3 H, s). ¹³C NMR (125 MHz, CDCl₃): δ /ppm = 165.37 (C), 162.82 (C), 159.83 (C), 158.94 (CH), 151.64 (CH), 149.07 (C, d, J = 241.2 Hz), 148.49 (CH), 142.49 (C), 135.04 (CH), 134.20 (C, d, J = 2.7 Hz), 133.75 (C), 132.45 (C), 129.35 (CH), 128.27 (C, d, J = 10.7 Hz), 127.03 (CH), 123.80 (CH), 114.88 (CH, d, J = 20.6 Hz), 113.94 (CH, d, J = 7.2 Hz), 112.41 (CH), 109.03 (CH), 62.34 (CH₂), 54.90 (CH₂), 52.64 (CH₂), 45.67 (CH₃). IR: ν_{\max} = 3395w, 3298w, 2933w, 2795w, 1642m, 1627m, 1581s, 1553m, 1533s, 1506m cm⁻¹. HRMS calculated for C₂₈H₂₉FN₇O, [M + H]⁺, 498.2418; found 498.2419, Δ = 0.2 ppm.

4-((4-Methylpiperazin-1-yl)methyl)-N-(3-((4-(pyridin-3-yl)pyrimidin-2-yl)amino)-4-(trifluoromethoxy)phenyl)benzamide 22. Purified by column chromatography (94 : 5 : 1 CH₂Cl₂-MeOH-conc. NH_{3(aq)}) to give the title compound (31 mg, 28%) as an off-white solid; mp 198–201 °C. Rt 4.01, [M + H]⁺ m/z = 564.2. R_f 0.21 (94 : 5 : 1 CH₂Cl₂-MeOH-conc. NH_{3(aq)}). ¹H NMR (600 MHz, CDCl₃): δ /ppm = 9.25 (1 H, d, J = 1.8 Hz), 9.13 (1 H, d, J = 2.1 Hz), 8.70 (1 H, dd, J = 4.7 and 1.5 Hz), 8.61–8.58 (1 H, m), 8.56 (1 H, d, J = 5.1 Hz), 8.05 (1 H, s), 7.85 (2 H, d, J = 8.2 Hz), 7.56 (1 H, s), 7.45 (2 H, d, J = 8.2 Hz), 7.44 (1 H, dd, J = 7.9 and 4.7 Hz), 7.33 (1 H, dd, J = 8.8 and 2.1 Hz), 7.28–7.25 (2 H, m), 3.57 (2 H, s), 2.49 (8 H, br s), 2.30 (3 H, s). ¹³C NMR (150 MHz, CDCl₃): δ /ppm = 165.51 (C), 162.86 (C), 159.71 (C), 158.93 (CH), 151.65 (CH), 148.51 (CH), 142.90 (C), 137.06 (C), 135.12 (CH), 133.99 (C), 133.51 (C), 132.80 (C), 132.40 (C), 129.35 (CH), 127.04 (CH), 123.80 (CH), 121.15 (CH), 120.74 (C, q, J = 259.1 Hz), 113.53 (CH), 111.85 (CH), 109.29 (CH), 62.46 (CH₂), 55.07 (CH₂), 53.07 (CH₂), 45.97 (CH₃). IR: ν_{\max} = 3439w, 3411w, 2939w, 2805w, 1665w, 1647w, 1607m, 1580m, 1556m, 1524s cm⁻¹. HRMS calculated for C₂₉H₂₉F₃N₇O₂, [M + H]⁺, 564.2335; found 564.2331, Δ = -0.7 ppm.

Acknowledgements

We would like to acknowledge the EPSRC (EP/F069685/1) and Pfizer Global R&D (MDH), the BP 1702 Chemistry Professorship (SVL) and the Royal Society (IRB) for funding. We would

also like to thank Pfizer Global R&D for performing the biological screening of the compounds made during this project.

Notes and references

- 1 J. Wegner, S. Ceylan and A. Kirschning, *Chem. Commun.*, 2011, **47**, 4583; B. P. Mason, K. E. Price, J. L. Steinbacher, A. R. Bogdan and D. T. McQuade, *Chem. Rev.*, 2007, **107**, 2300; P. Watts and C. Wiles, *Org. Biomol. Chem.*, 2007, **5**, 727.
- 2 D. Webb and T. F. Jamison, *Chem. Sci.*, 2010, **1**, 675; J. Wegner, S. Ceylan and A. Kirschning, *Adv. Synth. Catal.*, 2012, **354**, 17.
- 3 M. Baumann, I. R. Baxendale and S. V. Ley, *Mol. Diversity*, 2011, **15**, 613; D. L. Browne, B. J. Deadman, R. Ashe, I. R. Baxendale and S. V. Ley, *Org. Process Res. Dev.*, 2011, **15**, 693; C. F. Carter, H. Lange, D. Sakai, I. R. Baxendale and S. V. Ley, *Chem.-Eur. J.*, 2011, **17**, 3398; C. J. Smith, N. Nikbin, S. V. Ley, H. Lange and I. R. Baxendale, *Org. Biomol. Chem.*, 2011, **9**, 1938; M. D. Hopkin, I. R. Baxendale and S. V. Ley, *Chim. Oggi*, 2011, **29**, 28; D. L. Browne, M. Baumann, B. H. Harji, I. R. Baxendale and S. V. Ley, *Org. Lett.*, 2011, **13**, 3312; A. Polyzos, M. O'Brien, T. P. Petersen, I. R. Baxendale and S. V. Ley, *Angew. Chem., Int. Ed.*, 2011, **50**, 1190; J. T. Hodgkinson, W. R. J. D. Galloway, S. Saraf, I. R. Baxendale, S. V. Ley, M. Ladlow, M. Welch and D. R. Spring, *Org. Biomol. Chem.*, 2011, **9**, 57; L. J. Martin, A. L. Marzinzik, S. V. Ley and I. R. Baxendale, *Org. Lett.*, 2010, **13**, 320; C. J. Smith, C. D. Smith, N. Nikbin, S. V. Ley and I. R. Baxendale, *Org. Biomol. Chem.*, 2011, **9**, 1927; M. Baumann, I. R. Baxendale, M. Brasholz, J. J. Hayward, S. V. Ley and N. Nikbin, *Synlett*, 2011, 1375; M. O'Brien, N. Taylor, A. Polyzos, I. R. Baxendale and S. V. Ley, *Chem. Sci.*, 2011, **2**, 1250; P. Koos, U. Gross, A. Polyzos, M. O'Brien, I. Baxendale and S. V. Ley, *Org. Biomol. Chem.*, 2011, **9**, 6903; S. L. Bourne, P. Koos, M. O'Brien, B. Martin, B. Schenkel, I. R. Baxendale and S. V. Ley, *Synlett*, 2011, 2643; S. Kasinathan, S. L. Bourne, P. Tolstoy, P. Koos, M. O'Brien, R. W. Bates, I. R. Baxendale and S. V. Ley, *Synlett*, 2011, 2648; K. A. Roper, H. Lange, A. Polyzos, M. B. Berry, I. R. Baxendale and S. V. Ley, *Beilstein J. Org. Chem.*, 2011, **7**, 1648.
- 4 H. Lange, C. F. Carter, M. D. Hopkin, A. Burke, J. G. Goode, I. R. Baxendale and S. V. Ley, *Chem. Sci.*, 2011, **2**, 765.
- 5 J. Zimmermann, *Eur. Pat.*, 564 409, 1993.
- 6 J. Zimmermann, *US Pat.*, 5 521 184, 1996.
- 7 B. J. Deadman, M. D. Hopkin, I. R. Baxendale and S. V. Ley, *Org. Biomol. Chem.*, DOI: 10.1039/C2OB27003J.
- 8 I. R. Baxendale, C. M. Griffiths-Jones, S. V. Ley and G. K. Tranmer, *Synlett*, 2006, 427.
- 9 J. G. Lombardino, *US Pat.*, 4 623 486, 1986.
- 10 Solution phase bases were not desirable since any excess would be trapped onto the supported acid in the subsequent catch and release purification, possibly in preference to the product. This would undoubtedly lead to a contaminated product stream.
- 11 M. Tomoi, Y. Akada and H. Kakiuchi, *Makromol. Chem., Rapid Commun.*, 1982, **3**, 537; Y. Shai, K. A. Jacobson and A. Patchornik, *J. Am. Chem. Soc.*, 1985, **107**, 4249.
- 12 Y. Yoshida, S. Ishii and T. Yamashita, *Chem. Lett.*, 1984, **13**, 1571; Y. Yoshida, S. Ishii, M. Watanabe and T. Yamashita, *Bull. Chem. Soc. Jpn.*, 1989, **62**, 1534.
- 13 Available from Biotage AB. <http://www.biotage.com>
- 14 N. Hird and B. MacLachlan, in *Laboratory Automation in the Chemical Industries*, ed. D. G. Cork and T. Sugawara, Marcel Dekker, Inc., New York, 2002, ch. 1, pp. 1–40.
- 15 C. Mauger, O. Buisine, S. Caravieilhés and G. Mignani, *J. Organomet. Chem.*, 2005, **690**, 3627; J. A. Coggan, E. L. Moore and B. J. Worfolk, *US Pat.*, 7 563 932, 2009.
- 16 W.-S. Huang and W. C. Shakespeare, *Synthesis*, 2007, 2121.
- 17 M. Kranenburg, Y. E. M. van der Burgt, P. C. J. Kamer, P. W. N. M. van Leeuwen, K. Goubitz and J. Fraanje, *Organometallics*, 1995, **14**, 3081.
- 18 Y. Guari, G. P. F. van Strijdonck, M. D. K. Boele, J. N. H. Reek, P. C. J. Kamer and P. W. N. M. van Leeuwen, *Chem.-Eur. J.*, 2001, **7**, 475; Y. Guari, D. S. van Es, J. N. H. Reek, P. C. J. Kamer and P. W. N. M. van Leeuwen, *Tetrahedron Lett.*, 1999, **40**, 3789.
- 19 V. A. Stenger, *J. Chem. Eng. Data*, 1996, **41**, 1111.
- 20 D. S. Surry and S. L. Buchwald, *Angew. Chem., Int. Ed.*, 2008, **47**, 6338.
- 21 B. P. Fors, D. A. Watson, M. R. Biscoe and S. L. Buchwald, *J. Am. Chem. Soc.*, 2008, **130**, 13552.
- 22 M. R. Biscoe, B. P. Fors and S. L. Buchwald, *J. Am. Chem. Soc.*, 2008, **130**, 6686; D. Maiti, B. P. Fors, J. L. Henderson, Y. Nakamura and S. L. Buchwald, *Chem. Sci.*, 2011, **2**, 57.
- 23 W. Szczeppek, W. Luniewski, L. Kaczmarek, B. Zagrodzki, D. Samson-Lazinska, W. Szelejowski and M. Skarzynski, *World Pat.*, 2006 071 130, 2006.
- 24 I. R. Baxendale, S. C. Schou, J. Sedelmeier and S. V. Ley, *Chem.-Eur. J.*, 2010, **16**, 89.
- 25 Y.-F. Liu, C.-L. Wang, Y.-J. Bai, N. Han, J.-P. Jiao and X.-L. Qi, *Org. Process Res. Dev.*, 2008, **12**, 490.
- 26 D.-Y. Kim, J.-G. Kim, D.-J. Cho, G.-Y. Lee, H.-Y. Kim, S.-H. Woo, W.-C. Bae, S.-A. Lee and B.-C. Han, *World Pat.*, 2004 099 186, 2004.
- 27 H. M. Buerger, G. Caravatti, J. Zimmermann, P. W. Manley, W. Breitenstein and M. A. Cudd, *World Pat.*, 2002 022 597, 2002.